SEISMIC RESPONSE OF REDUCED SCALE SOIL RETAINING WALL AT VARYING BACKFILL DENSITY

A Thesis Submitted in Fulfilment of the Requirement for the Award of

the Degree of

MASTERS OF ENGINEERING

IN

INFRASTRUCTURE ENGINEERING

submitted by

MANIK SHARMA

801723012

under the supervision of

Dr. Aditya Parihar

Assistant Professor

Department of Civil Engineering

T.I.E.T, Patiala, Punjab

DEPARTMENT OF CIVIL ENGINEERING

THAPAR INSTITUTE OF ENGINEERING AND TECHNOLOGY

(A DEEMED TO BE UNIVERSITY), PATIALA, PUNJAB

JULY 2019

SEISMIC RESPONSE OF REDUCED SCALE SOIL RETAINING WALL AT VARYING BACKFILL DENSITY

by

MANIK SHARMA

801723012

A thesis submitted in partial fulfilment

of the requirement for the degree of

Master of Engineering

in Infrastructure Engineering

July, 2019

DECLARATION

I, Manik Sharma, hereby declare that this thesis entitled **"Seismic Response of Reduced Scale Soil Retaining Wall at Varying Backfill Density "** is an reliable record of my study carried out as requirements for the award of degree of **Master of Engineering** in **Infrastructure Engineering** in the Civil Engineering Department, Thapar Institute of Engineering and Technology , Patiala under the supervision of **Dr. Aditya Parihar, Assistant Professor,** Department of Civil Engineering, Thapar Institute of Engineering and Technology , Patiala during July 2018 to July 2019 . This matter exemplify in this report has not been submitted in part or full to any other university or institute for the award of any degree.

Date: 15/07/2019

Place: PATIALA

Manik Sharma

Roll No. :801723012

This statement is to certify that the student concerned is correct and true to the prime of my knowledge and opinion.

15/7/2019

DR. Aditya Parihar

Assistant Professor

Department of Civil Engineering

Thapar Institute of Engineering and Technology , Patiala

ACKNOWLEDGEMENT

At first, I wish to express my deep sense of gratitude to my guide Dr. Aditya Parihar, Assistant Professor, Thapar Institute of Engineering and Technology, Patiala for taking keen interest and guiding me throughout my M.E. thesis work. His vital comments, constructive suggestions and constant inspiration have been instrumental in completing my work.

My sincere thanks also goes to Dr. Rajesh Pathak for his valuable help in setting up the machinery required in completing my thesis. I want to thank you for your vital help and your constant and priceless recommendations time to time.

I would like to express my special gratitude and thanks to Dr. Shweta Goyal, Dr. Naveen Kwatra and Ms. Priya for allowing me to use the valuable equipments and helping in assembling the experimental setup. Without their help and cooperation, I wouldn't have been able to complete the thesis.

I would like to thank my parents and my brother for always believing in me and always encouraging me to pursue even bigger dreams whilst showing their full support. I will forever be grateful for their love.

It gives me immense pleasure to acknowledge the help and encouragement rendered by my friends Ajay, Gopesh, Shubham, Suneha and Venus who were always there for me during the hardest of times making me positive and ecstatic.

I would also like to thank Mrs. Ranjana and staff at the geotech lab that always had a helping hand whenever I needed it with their constant support and cooperation.

To end with, my 'pranams' to THE LORD SHIVA for having kept me in serenity and good health which paved way for the successful completion of my thesis.

ABSTRACT

In this study, the shaking table tests on small scale model of soil retaining walls are done in the laboratory. The seismic response of three retaining wall models is studied by performing a series of laboratory experiments under the influence of changing backfill relative density by applying different acceleration amplitudes. The background of the study, literature on the study and attempted study is presented in detail. The small scale model construction, materials used, instrumentation and results are also presented in detail in this study.

Three types of wall: rough, frictionless and rough with surcharge walls are constructed to different relative densities and these walls are tested at three different excitations. The static and dynamic displacement of these walls with the change in backfill relative densities is also recorded and presented in this study. The acceleration amplification comparison is also made between the base and top of the backfill densities of different retaining walls. It is observed that the dynamic displacement decreases with increase in relative density of backfill. The displacement in surcharge wall is recorded as maximum. The acceleration amplification increases with increase in relative density of backfill at higher acceleration amplitudes whereas it decreases with increase in relative density of backfill at lower excitation. The acceleration amplification is most pronounced in case of frictionless wall as compared to rough wall with and without surcharge. The displacement in frictionless wall is less than rough wall with surcharge but more than rough wall without surcharge.

The results obtained from this study are helpful in understanding the relative performance of soil retaining walls constructed when subjected to higher base excitation for the range of relative density employed in the testing program.

TABLE OF CONTENTS

CHAPTER 1 INTRODUCTION 1

1.1 General Background 1

1.2 Objectives of the Study 4

1.3 Organization of the Thesis 5

CHAPTER 2 LITERATURE REVIEW 6

2.1 Existing Literature 6

2.2 Summary 21

CHAPTER 3 METHODOLOGY 23

3.1 Introduction 23

3.2 Materials used in Experiment 25

3.2.1 Backfill Material 25

3.2.2 Retaining Wall 28

3.2.3 Sensors 30

3.3 Equipment Setup 32

3.3.1 Shaking Table 32

3.3.2 Metal Frame 33

3.3.3 Sand Raining Sieve 35

3.4 Model Construction 37

3.5 Similitude Laws 42

3.6 Root Mean Square Acceleration ($\boldsymbol{arms}$) 44

3.7 Displacement by Whitman & Liao (1980) Method 44

CHAPTER 4 RESULTS AND DISCUSSION 46

4.1 Introduction 46

4.2 Response of rough wall 46

4.2.1 Effect of backfill density 46

4.2.2 Effect of base acceleration intensity on dynamic response 55

4.2.3 Effect of surcharge on top of backfill 62

4.2.4 Effect of interface friction 68

4.3 Comparisons between 3 model walls 70

4.3.1 Amplification Ratio Comparison 70

4.3.2 Displacement Comparison 71

4.3.3 Acceleration Amplification Comparison with Literature Present 72

4.4 Theoretical Displacement using Whitman & Liao (1980) 73

CHAPTER 5 CONCLUSIONS AND SUGGESTIONS 76

5.1 Conclusions 76

5.2 Comparison with Literature 77

5.3 Suggestions 78

REFERENCES 79

LIST OF FIGURES

Figure 3.1: Flow Chart.....24

Figure 3.2: Grain Size Distribution.....25

Figure 3.3: Direct shear test result (R.D. = 35%, 45% and 55%).....27

Figure 3.4: 12 mm thick 3 panelled staged wall......29

Figure 3.5:12 mm thick 3 panelled reduced friction wall. 29

Figure 3.6: AG Measurematics Alternating Current LVDT......30

Figure 3.7: Micron Optics Accelerometer os7100. 31

Figure 3.8: Shake Table assembly......33

Figure 3.9: Metal Frame. 34

Figure 3.10: Custom made sieve of size 1.75 mm......35

Figure 3.11: Calibration Graph for Sand Pluviation......36

Figure 3.12: Schematic of the Shaking Table Model Assembly......38

Figure 3.13: Sunmica Affixed to the Walls of Shake Table. 39

Figure 3.14: Plywood Base of the Shaking Table......39

Figure 3.15: Attached LVDT's to the metal frame. 41

Figure 4.1: Displacement Response at base acceleration level 1. 47

Figure 4.2: Displacement Response at base acceleration level 2. 48

Figure 4.3: Displacement Response at base acceleration level 3. 49

Figure 4.4: Acceleration time history at top of wall (acceleration level 1, R.D. 55%)......50

Figure 4.5: Acceleration time history at top of wall (acceleration level 1, R.D. 35%)......50

Figure 4.6: Acceleration time history at top of wall (acceleration level 2, R.D. 55%)......51

Figure 4.7: Acceleration time history at top of wall (acceleration level 3, R.D. 45%)......52

Figure 4.8: Acceleration time history at top of wall (acceleration level 3, R.D. 35%)......52

Figure 4.9: Acceleration Level 1 Base Time History. 56

Figure 4.10: Acceleration 2 Base Time History. 56

Figure 4.11: Acceleration Level 3 Base Time History. 57

Figure 4.12: *Displacement Response at R.D. 55%.*.....58

Figure 4.13: *Displacement response at R.D. 45%.*.....58

Figure 4.14: *Displacement response at R.D. 35%.*.....59

Figure 4.15: Displacement Response at R.D. 55% (surcharge)......62

Figure 4.16: Displacement Comparison at Base Acceleration Level 1 (surcharge)......63

Figure 4.17: Displacement Comparison at Base Acceleration Level 2 (surcharge)......64

Figure 4.18: Displacement Comparison for Base Acceleration Level 3 (surcharge). 65

Figure 4.19: Acceleration time history at top of wall (acceleration level 1, R.D. 55%, surcharge)......66

Figure 4.20: Displacement Response at Base Acceleration Level 2 (reduced friction)......69

Figure 4.21: Displacement Comparison for Base Acceleration Level 2 (three walls)......71

LIST OF TABLES

Table 3.1: Index properties of test sand......26

Table 3.2: Similitude laws for shaking table model test.....43

Table 4.1: Amplification Ratio for Base Acceleration 1......53

Table 4.2: Amplification Ratio for Base Acceleration 2......54

Table 4.3: Amplification Ratio for Acceleration 3......54

Table 4.4: *Amplification Ratio at R.D. 55%.* 60

Table 4.5: Amplification Ratio at R.D. 45%......61

Table 4.6: Amplification Ratio at R.D. 35%......61

Table 4.7: Amplification Ratio for R.D. 55%. 67

Table 4.8: Amplification Ratio Comparison at 55% R.D. 68

Table 4.9: Amplification Ratio for Base Acceleration Level 2 (reduced friction)......70

Table 4.10: Amplification Ratio Comparison for Base Acceleration Level 2 (3 walls). 71

Table 4.11: Theoretical Maximum Displacement at Different Base Accelerations 74

LIST OF SYMBOLS

Hz	Hertz
kN	Kilo Newton
M	Magnitude of Earthquake
M_w	Moment Magnitude of Earthquake
SP	Poorly Graded Sand
Cc	Coefficient of Curvature
Cu	Coefficient of Uniformity
e_{max}	Maximum Void Ratio
e_{min}	Minimum Void Ratio
Φ	Angle of Internal Friction
τ	Shear Stress
σ	Normal Stress
λ	Model Parameter Time
t_m	Geometric Scale Factor
σ_m	Model Parameter Stress
a_{rms}	Root Mean Square Acceleration
λ_0	Average Intensity of Acceleration
$\bar{d}_{perm}$	Maximum Velocity
v_{max}	Maximum Permanent Displacement
a_{max}	Maximum Acceleration
a_y	Yield Acceleration

LIST OF ABBREVIATIONS

SRW	Segmental Retaining Wall
RD	Relative Density
M-O	Mononobe – Okabe
IS/BIS	Bureau of Indian Standard
LVDT	Linear Variable Differential Transformer
FBG	Fibre Bragg Grating
RMSA	Root Mean Square Acceleration

CHAPTER 1
INTRODUCTION

1.1 General Background

Constantly increasing infrastructure demands, increase in population and vehicular traffic, and increased awareness regards earthquake preparedness has led to refined design practises for retaining structures amongst other important structures. Retaining walls is designed to resist the lateral thrust from the retained earth. The earth thrust could be due to its own weight and surcharge. Permanent deformation of retaining structures has been caused due to many historical earthquakes. Some of them causing heavy damage and others cause damage almost negligible. Disastrous physical and economic consequences have been faced by mankind when retaining structures have collapsed during earthquakes. Retaining walls are vulnerable to failure if their responses under static and dynamic conditions are not properly predicted and designed accordingly. Therefore, while designing retaining walls, stress and displacement criteria become important. Magnitude and distribution of displacement of wall and earth pressure under static and dynamic conditions is required for the design and analysis of retaining wall.

Assessment of the performance of retaining soil structures exposed to seismic loading, whether in the laboratory model tests or through numerical analysis or in the field, provide insight into the expected behaviour to be considered in design. Several studies on them under static and working conditions have been stated (Edgar et al., 1989; Wong et al., 1994; Bathurst et al., 2005). Studies on their dynamic behaviour have also been carried out by various scientists for past 25 years (Nova-Roessig and Sitar, 2006; Cai and

Bathurst, 1995; Richardson and Lee, 1975; Bathurst and Hatami, 1998). For the better understanding of how the retaining walls behave during an earthquake, performance of the physical models can be studies under the influence of cyclic ground shaking conditions.

The use of modular or segmental retaining walls (SRW) has increased in recent times. The segments may be made of concrete block units embedded with polymeric reinforcements. For the present study wooden segmental panels are used for the small scale model of retaining wall. Several studies on SRW have been conducted by many researchers Simac and Bathurst (1994), in Europe, Scandinavia and Australia.

Shaking table tests can be done on comparatively larger assemblies and the magnitudes of response parameters with the reaction of the tests can be physically observed. Shaking table tests are conducted mainly using the reduced scale models (Bathurst et al., 2001; Panah et al., 2015). In the present study, the shaking table had a frequency of 0.779 Hz, 0.795 Hz and 0.806 Hz with a variable seismic loading of 0.6 g to 2 g. The height of the retaining wall used for the present study is 0.4 m.

The density of the soil and the amount of compaction greatly affects the seismic response of the retaining walls. The properties of soil play a vital role in this response. One of the chief controlling factors in the design of the retaining wall is the relative density of the backfill soil. According to Sakaguchi (1996), the density of the backfill has more effect as compared to the tensile strength of the reinforcement on the response of the retaining wall. According to him, for improving the performance of walls subjected to both small and large base accelerations, the geosynthetic strength has little effect on. The performance of retaining wall relies mainly on sand-geosynthetic friction. The stiffness of the reinforced retaining wall can be changed by the density of the soil used; therefore,

during construction the characteristic of compaction is a significant factor in monitoring the performance of a reinforced retaining wall. Lee and Wu (2004) presented a combination of 10 totally instruments case histories of flexible faced reinforced soil structures with varying backfill type, geometry, relative density and reinforcement. The study indicated that the relative density and backfill type play vital role on the performance response of the retaining walls as compared to reinforcement length and reinforcement type which only have a minor effect on the performance characteristics of retaining wall. In terms of lateral movement of the wall face, crest settlement, surcharge pressure at failure and reinforcement strain, the relative density of the backfill and the soil type plays a vital role. Backfill densities were also varied by Lee et al. (1973) for testing the small scale models of retaining walls. Tests were done by him at 2 densities of backfill sand: dense (63% RD and loose (20% RD). For loose backfill sand, slight difference in collapse heights was noted as compared to in case of dense backfill sand.

For presenting the effect of proctor density on the linear deformations of facing in the retaining wall, Bathurst and Karpurapu (1992) conducted a study. It was observed that with the increase in proctor density from 80% to 95%, the linear deformations reduced by about 30%.

In present study, attempt is made to assess parameters affecting response of retaining walls under high intensity seismic load. The soil wall models are constructed at different backfill densities of 35%, 45% and 55% and their response is recorded after and before they are subjected to different base excitations. The response of the retaining walls is recorded in terms of numerous parameters such as linear displacement of facing, acceleration response and acceleration amplification with the increase in elevation. Tests are carried out using a sinusoidal motion by carrying out tests on uni-axial shaking table, series of shaking table tests are planned and carried out to clearly bring about the effect of

changing base acceleration, changing backfill densities on the seismic performance of rough, frictionless and rough wall with surcharge.

1.2 Objectives of the Study

The main objectives to be accomplished in the thesis are as under:

- To set up the shaking table model assembly for performing the desired experiments on it.
- To select and set up the small scale retaining wall with respect to the scaling factors keeping in mind the aspects of the shaking table and the area of the backfill.
- To determine the height of fall required to accomplish the chosen densities of backfill at which the experiments are to be performed.
- To record the displacement response (both the static displacement before the application of seismic load and dynamic displacement after the application of seismic load at the top and middle of the walls) of three different walls i.e. rough wall, frictionless wall and rough wall with surcharge at varying backfill relative densities of 35%, 45% and 55% and at three varying base acceleration excitation.
- To register the acceleration response at the top of the backfill corresponding to three base excitations and three walls at varying relative densities of backfill at 35%, 45% and 55%.
- To compute the acceleration amplification in the backfill at varying relative densities with the increase in elevation from the base of the backfill.
- Compare the acceleration amplification for different base acceleration amplitudes of different walls at varying R.D. of backfill.
- To carry out the comparison of lateral static and final dynamic displacement between all the three walls at the top and middle.

- To compute the comparison of lateral displacement between the rough wall when used with and without surcharge.
- To compute the theoretical displacements at the top of three walls at varying base acceleration amplitudes using Whitman & Liao (1980) method by assuming the maximum value of velocity of base acceleration.
- To carry out the difference between the experimental and theoretical displacement of the rough retaining wall at the top of the wall.

1.3 Organization of the Thesis

The study of the seismic reaction of the retaining walls at varying backfill R.D. and varying base acceleration amplitudes is presented in this research work. The whole work of the thesis is presented in 6 chapters. Brief symposium about the structure of thesis is given below.

The chapter 1 of the thesis gives a background, the main objectives of the study along with an organization of the thesis. In Chapter 2, a comprehensive literature review of each topic of importance has been presented along with the results and discussions presented by different researchers on same and related topics. In Chapter 3 i.e. methodology, a detailed discussion about materials that were used in the study, equipment and instrument that were set up and used during the study, assembling the model and its construction is presented. In the Chapter 4, outcomes of the experiments with a detailed discussions about the results recorded is presented accompanied with graphs and tables. In the last chapter i.e.5th, brief conclusions generated from the recorded results and suggestions inferred from the results are given.

CHAPTER 2
LITERATURE REVIEW

2.1 Existing Literature

Numerous researchers have conducted extensive experimental and numerical studies to assess the factors affecting dynamic response of retaining wall.

Prakash Shamsher (1981), discussed in detail the changing pressures as well as the displacements under went by retaining walls during earthquakes. A method to calculate seismic coefficient to be used in the method proposed by Mononabe has been given and increments in active earth pressures have also been correlated with peak ground velocity. Detailed examination of the position of appliance of the dynamic increment is also given in this study. Three methods of computing the displacements of rigid retaining walls has been provided i.e. a) Newmark's approach of sliding block, b) calculation of translation only and c) calculation of displacements as a result of rotation of wall.

For this study, large quantities of experimental data concerning the magnitude of the total earth pressure during vibrations have been collected. Several experimentations have been performed on small scale model of walls to comprehend their physical behaviour.

On the basis of the observations and data recorded, this study concluded that the fluctuations of the earth pressure during the earthquake became greater when closer to the ground surface. The earth pressure recorded during the earthquake was very similar to those appeared on the ground displacement record. The centre of dynamic earth pressure increment has been shown to act at 0.55 H and 0.45 H over the base of flexible and rigid walls respectively.

Cilingir U et al. (2011), conducted both the Finite Element analyses and centrifuge testing aimed at the investigation of an anchored sheet pile wall in dry sand on application of seismic Anchor beam connected by two tie rods have been used to tie model wall with the backfill. Miniature piezoelectric accelerometers were used in measuring the accelerations of the anchor beam, the soil around the wall and the sheet pile wall. The bending moments induced in the walls were measured by strain gauges at 5 different locations. The anchor forces were measured by load cells. Comparison was made between the results obtained from centrifuge tests with 2D, plane strain FE analyses.

The centrifuge tests were carried out with an acceleration of 0.80 g on aluminium sheet pile models of wall of size 9.6 m high and 0.12 m thick was used. It was observed form this study that a composite soil-structure interface exists between the anchor beams, the backfill soil. The acceleration time histories recorded showed significantly similar results as computed by FE analyses. It was also seen that the earthquake loading results in accumulation of wall deformations and permanent bending strains. The highest bending moment was recorded at about two thirds of the excavation depth.

Park R. et al. (1979), conducted the study on dynamic analyses of structures responding elastically and in elastically to seismic ground motions, earthquake code factors and ground motions. Experimental and analytical investigation of the assemblies, concrete elements and earth retaining structures subjected to earthquake type loading was also carried out. The reinforced concrete shear walls coupled by deep diagonally reinforced coupling beams have also been investigated. An experimental test was done to verify the Richard- Elms model using small scale prototype tests on a shaking table. Further experimental work were carried out on the basic mechanism of failure of retaining wall by recording the response to a smooth sinusoidal acceleration input corresponding to a scaled earthquake record.

Wood J.H. (1975), conducted this research to describe the appliance of linear elastic theory for the estimation of the earthquake provoked soil pressures on a part which formed wall of the structure power station which had foundation on a rock. This research describes the appliance of a numerous appraise methods to calculate the earthquake provoked pressures on a soil retaining wall. The analytical solution was evaluated assuming that the prototype problem could be characterised by an estimated equivalent rectangle of soil with L/H ratio of 1.67. A finite element technique was used in calculating the earthquake provoked wall pressures on a rigid wall case. The response spectrum method was used in computing the maximum earthquake induced pressure distribution.

The Mononobe-Okabe method gave satisfactory results for many wall structures but to produce satisfactory results the basic supposition of adequate wall displacement to create a fully plastic stress state in the soil must be reassured. In case of rigid walls, the Mononobe-Okabe method is not suitable. The inertia forces acting on the structure which causes displacements should also be measured.

Oldecop Luciano, Zabala Francisco and Almazan Jose Luis (1996), carried out a shaking table test on a 65 cm high gravity retaining wall arranged in a 3 m long tank with glass sides. Wall was backfilled with 10 cm thick clean sand. Horizontal and vertical wall displacements, accelerations of shaking table and wall and earth pressure magnitude and distribution were measured in this research.

The wall mass was variable by adding weights of 30 kg each. The friction on the wall vertical face-backfill interfaces and on the wall base foundation was increased by bonding sand with epoxy resin. The frequency of excitation motion was fixed at 10 Hz and its

duration at 16 seconds. At the starting, the acceleration amplitude was kept at 0.25 g which was increased in 0.1 g steps in successive motion.

The results showed that the structure behaviour had two well defined stages that were, a first stage of 10.5 s duration with low rate of permanent displacement accumulation and a second stage of duration 5.5 s with high rate of permanent displacement accumulation.

In the first stage of wall response, rocking plays an important role. Rocking is, at least for the tested structures the overestimation occurrence in the mathematical models. Zabrrabi model overcomes this problem of overestimation. There is a residual backfill thrust increase during the motion so that the final static thrust is greater than the initial value. It was also seen that the moving from first stage to second stage, the structure changed its behaviour.

Elms D. G. and Richards R. (1979), conducted the research on the design of the gravity retaining walls subjected to seismic excitation. The seismic behaviour of gravity retaining wall is investigated starting from Mononobe-Okabe study. The importance of including the wall inertia effects is also demonstrated. Exploration of sensitivity on changing various parameters is also investigated. An approximate expression is given to calculate the expected displacement. A design approach which needs to be followed is provided with.

From this study, it became clear that a gravity retaining wall subjected to small earthquake excitation will undergo permanent displacement. A gravity wall should therefore be detailed to allow some movement to take place, and it should be proportioned so that its deformation would be by sliding rather than tilting. When the movement of the wall occurs, it will be finite and calculable. Firstly, an allowable displacement should be specified and then the acceleration coefficients which depend

upon the seismic zones should be defined. In some cases, the design mass of the wall should also be taken care of as the results are sensitive to the low value of internal friction angle of backfill soil. This analysis is however restricted to gravity retaining walls with saturated backfill.

Mikola Roozbeh Geraili, Candia Gabriel and Sitar Nicholas (2016), performed a series of tests on model retaining walls with medium dense cohesion less backfill using centrifuge experiments to acquire a better knowledge of the allocation and level of seismic earth pressures. In this study, 2 series of centrifuge small scale tests were done. Models of 3 types of exemplar retaining wall were modelled in this study. The height of the models examined ranged from 6.1 to 9 m

The main objective of the study was to get a dependable measure of earth pressure and describe the ground motion. So, accelerometers were operated along with LVDT's for displacement measurement. LVDTs were placed in a special frame. Numerous shaking measures were pertained to the constructed models at 0.36 g centrifugal acceleration. Concluding, the data showed that seismic earth pressure rises with the M-O solution and the stationary earth pressure distribution which formed the higher assurance for the laboratory experiment results.

Cai Zhenqi and Bathurst Richard J. (1995), obtained the results on the finite element analysis of the active response of the retaining wall reinforced with geosynthetic and made with dry-stacked modular concrete blocks. A hysterical model was used in modelling the reinforcement material which is based on the cyclic load-extension experiments in the laboratory. The main analyses of the lateral wall displacement, tensile forces expounded in the reinforcement and cumulative interface shear force was carried out during the course of this study. The frequency range applied varied from 0.5 to 2 Hz.

The backfill soil properties were based on a typical granular backfill with friction angle of 35° and unit weight of 19 kN/m³. Polymeric geogrid reinforcement was used in the backfill soil. The peak acceleration of 0.125 g and 0.25 g was applied for continuous 30 second duration.

The interface shear force and relative displacement increased with an upsurge in the extent of base excitation during the simulated seismic events. Cumulative active tensile forces were observed in the reinforcement layers. Across the wall system, the prediction of horizontal acceleration showed that at the same time, the peak acceleration occurred.

Simonelli Armando L et al. (1998), obtained the outcomes of shaking table test on a small scale model of earth retaining wall. Results obtained by the numerical methods were used in making comparisons based on a sliding block model (Newmark, 1965) and experimental results. A flexible shear stack of size 1.2 m high, 4.8 m long and 1 m wide retaining wall model was tested along with backfill soil. A frequency of 5 Hz was used at the small scale model of retaining wall. The integration i.e. numerical of the acceleration excitation time history graphs was used in computing the displacements in the ground and wall. The comparative horizontal displacement in between the wedge of the soil and wall is assumed to be zero for computing the soil and wedge accelerations. Leighton Buzzard Sand was used as a backfill material which was tested as fine to medium, dry and cohesion less soil. The main objective of the research work was to find the kinematics of the retaining wall, the computation of the boundary acceleration of the soil-wall system and their relative displacement measurements. The movements of the top and bottom of the wall are recorded to study the behaviour of the wall using accelerometers and displacement sensors. A frequency of 5 Hz was adopted to carry out tests with amplitude increasing from 0 to 10 for first 10 cycles, then remained constant for next 20 cycles and

then decreased from maximum to zero for last 10 cycles. The acceleration amplitude varied from 0.175 g to 0.411 g in the total of nine tests performed.

After the comparison was made between the Newmark Model and Zarrabi-Kashani model (1979), it confirmed the effectiveness of the rigid block model. The rigid block model showed the same characteristics as that of the kinematics of the sliding phenomenon. It also showed that the analytical method is somewhat conservative but reliable. The numerical methodologies originated from the Newmark Model could be used effectively in new performance centred design models and could be counted as a reliable predicting tool.

Bathurst R.J., Hatami K., and M.M. El-Emam (2005), carried out this study to investigate the amplification of the acceleration in the soil backfill of the retaining wall models which were reinforced and horizontal ground acceleration was applied on them. Using the numerical models demonstrating the propped-panel retaining walls at 3 varying heights, the influence of the wall height on the vertical distribution and magnitude of acceleration in the backfill was inspected. A changing amplitude harmonic motion was directed at the foundation level in most of the cases. In this study, the wall models examined were continuous propped concrete panel reinforced walls with cohesion less granular backfill. Using an actual earthquake record, a scaled accelerogram and a variable amplitude harmonic motion were input to the models.

3 distinct wall heights i.e. 3, 6 and 9 m were examined. For minimizing the amount of variable parameter in analysis; a continuous stiffness soil model was worked for the study. The reinforced soil backfill was constructed in layers with each panel supported horizontally by external rigid supports during construction. Two different ground motion

acceleration values i.e. 0.2 g and 0.4g were applied at the foundation level for acceleration amplification of the backfill.

Generally, through the surge in the elevation from the foundation level of the backfill, the acceleration amplification increased in the backfill for each wall model. Acceleration amplification also increased with the increase in the height of the retaining wall for a given input-to-structure frequency ratio. With the decrease in the immediacy of the input acceleration and the base acceleration of the structure, the acceleration amplification increased. For walls with height more than 3 m, lowering the ground motion intensity resulted in increase in the acceleration amplification of the backfill. Acceleration amplification also increased with decrease in the backfill damping ratio value. The kind of soil model i.e. linear or non-linear elastic was also supposed to have a considerable effect on the upsurge or reduction in the acceleration amplification of the backfill soil in the retaining walls. In this study, a linear elastic-plastic soil was adopted. For this type of backfill, the acceleration amplification was considered to be large as compared to soil with nonlinear or strain- softening characteristics. In the case of backfills with less density, with strain and plastic behaviour, reduction of soil shear modulus reduced the capability of the backfill to amplify the straight acceleration up the height of the retaining wall. Due to this, significant amplification was observed in case of short walls with elevation less than 3 m.

Ling Hoe I., Liu Huabei and Mohri Yoshiyuki (2005), conducted a number of parametric findings on the behaviour of reinforced soil walls under construction and subjected to finite loading using a finite element procedure. Incorporation of a widespread plasticity soil model and bounding surface geosynthetic model was done by utilizing nonlinear numerical algorithms. The main variables of investigation included earthquake motion block interaction properties, reinforcement layout and soil properties under

monotonic and cyclic loading. The functioning of the wall was offered under variables of linear earth pressure, acceleration amplification, facing deformation and crest settlement.

A generalized plasticity model was used in expressing the foundation and backfill soil. 15 parameters were required for simulating cyclic loading in generalized plasticity model. Several earthquake motions including the 1995 Kobe earthquake, the 1994 Northridge earthquake, the 1940 El Centro were contemplated as contribution for the bottom case.

Minimal results were recorded due to reinforcement cyclic properties and block interaction behaviour. Almost negligible effects were noticed in case of interaction behaviour. Soil behaviour and reinforcement layout also affected the facing lateral displacement and the maximum force exerted by the reinforcement layer, it also emerged that the length had a lesser effect than the spacing in linear displacement and force exerted.

Latha G. Madhavi & Krishna A. Murali (2007), conducted laboratory tests on small scale reinforced retaining wall models mounted on shaking table and the influence of backfill relative density, base motion frequency and type of facing on the seismic response of retaining walls. Authors studied using 3 types of walls i.e. reinforced rigid faced wall, unreinforced rigid faced wall and wrap wall and tested them for seismic response at different backfill density for a small excitation of 0.1 g, while wrap faced walls were tested for both small and high excitation of 0.1 g and 0.2 g. The backfill density of the retaining walls was varied between 37- 87%. Displacement, acceleration and earth pressure measurements were done in study using sensors mounted at different heights of wall.

Displacement response of wrap faced wall suggested that effect of density is more pronounced, and that with higher elevation face deformations increase and accelerations

are amplified. It was also observed that variation in R.D. of backfill for lesser base excitations does not have much effect on the acceleration amplifications for varying model walls, while deformations were profound and they decrease with increasing R.D. of the backfill. Though, at higher base excitation, it was detected that the backfill R.D. considerably affects the response and there is slight increase in acceleration amplification while, the deformations decreased with the increasing in R.D. of backfill.

Guler Erol, Enunlu Ali K. (2009), conducted and presented a study on 1:2 reduced-scale model of soil retaining wall reinforced with geotextile reinforcement. The sinusoidal harmonic motions were applied using shaking table to 1.9 m tall models. Evaluation of acceleration amplifications and deformations in the wall facing was done in this study.

A uniaxial shaking table was used in this study which had frequency varying from 0-50 Hz was used for the study. SW-SM type of sand was used for the study which was well graded silty for the backfill. For the facing of the wall, concrete walls of size 100 * 100 * 200 mm were used. Sand layer was compacted by a plate compactor at every stage and was filled in 100 mm thickness

There was an increase in the highest amplification factor with increase in the elevation on the facing of the wall surface. In case of shorter reinforcements, the dynamic stresses in the reinforcement were recorded to be more. Models with shorter reinforcements also showed larger deformations as compared to models with larger reinforcements. Maximum tensile stress happened in areas which were near the failure surfaces foreseen by Rankine theory.

Nelson Anitha and Jayasree P.K. (2010), in this study, discussed the reaction of reinforced soil retaining walls with block facing in terms of reinforcement tensile force, lateral facing deflection and crest surface settlement when the retaining walls were

exposed to earthquake excitation applied by the means using finite element analysis package, PLAXIS V8. Form the study, it was noted that there is a significant effect of seismic loading on the response of the reinforced soil retaining walls and the design and analysis of these walls should be done with consideration of dynamic seismic loading in earthquake prone areas.

For this study, 2 different types of reinforced soil walls were considered: gabion faced wall and segmental walls. The response of gabion faced and segmental wall under the influence of seismic loading was analysed. Development of finite element model for the gabion faced and segmental reinforced soil wall was done. Performance evaluation of the different walls based on different materials used and geometric parameters was also done.

The wall was made for a horizontal highest acceleration of 0.2 g. the system of retaining wall included natural backfill which was to be retained by a 6m high wall. The facing of the wall was made of blocks and geotextile sheet reinforcement was used. Cohesive soil was used for the backfill of the retaining walls.

The highest linear displacement happened at the tip of the retaining wall and the tensile force was recorded maximum at the bottom most reinforcement in both the wall cases. Under the earthquake loading, the gabion faced retaining walls was found to perform at a higher level than cement concrete block faced reinforced retaining walls. In both the walls, the acceleration amplification increased as they went from bottom to top and increased in magnitude with the elevation of the wall. The backfill soil also affected the response of the wall as the deflection patterns for clay and sand were different. The results also established that the length of the reinforcement used in the backfill of the retaining wall plays an vital role in reducing the wall deformations to the minimum..

Zarnani Saman, El-Emam Magdi M. and Bathurst Richard J. (2011), in this study described a simple numerical FLAC model to compute the effects of earthquake excitations on retaining wall. The retaining wall models of size 1 * 1.4 * 2.4 m were made with a sand backfill of constant size. In one model, hinged toe wall was used and in other model, an idealized sliding toe was used. The material properties were determined in separate laboratory testing. This research briefly described two physical test models varied with respect to toe boundary conditions and numerical approach. Cohesion soil with internal friction angle of 51˚ and unit weight 15.7 kN/m³ was used for the study. Base accelerations of up to 0.35 g were applied on the hinged toe model wall.

From the research, it was concluded that a simple elastic-plastic model is adequate to calculate wall deformation, reinforcement load and footing. Both the numerical and physical modelling presented the distribution and magnitude of reinforcement association loads. Ground acceleration amplifications were found to be sensibly constant at about 1.1 at all the locations in the numerical model.

Conti R., Madabhushi G.S.P. and Viggiani G.M.B. (2012), conducted an experimental investigation of the embedded retaining walls under seismic loading. For this purpose, 9 tests were conducted on small scale models of soil retaining walls with dry sand backfill using centrifuge tests. Walls used were either propped at one level or cantilever near the top of the wall. The experimental tests were done at two centrifuge accelerations of .40 g and .80 g. Retaining wall models were made of aluminium alloy plates. Standard silica dry sand was used with angle of internal friction 32˚ and specific gravity of 2.65. Accelerometers and LVDT's were used in recording the accelerations at the top and bottom and lateral displacements in wall respectively. Seismic load was applied on the model of retaining wall for a continuous period of 32 seconds.

The experimental results showed that both the retaining wall models i.e. propped and cantilever showed permanent displacements on the rigid walls even for the accelerations smaller than critical values of acceleration.

Moss Robb Eric S., Noche Ron E. (2012), used a scale model of retaining wall made on a testing platform which was placed on a shake table of 1 g to compute the magnitude and distribution for the prototype soil conditions of seismic earth pressures. The study included the similitude scaling of the input time histories, dynamic properties of soil and wall dimensions. Initial soil structure interaction effects for the basement conditions were included in the experiments. A wall prototype of 3 m was used in conducting experiments by experiencing a large ground motion.

The main testing equipment consisted of a shake table with a flexible wall barrel mounted on it. The barrel wall was made of rubber membrane confined by kevlar straps. A mixture of water, fly ash, bentonite, and kaolinite were used in specific volume to reach the desired strength of the prototype. The frequency range of the shake table was 0.1 Hz to 50 Hz and it had a peak displacement of 25 mm.

After the study, the static stress conditions were found to be same as would have been probable for normally consolidated clay for a 3 m high model retaining wall. The calculated seismic earth pressure was same as calculated using the M-O method.

Latha G. Madhavi and Santhanakumar P. (2015), laid emphases on interpreting the seismic response on small scale models of rigid faced and modular block retaining wall reinforced with geosynthetic reinforced through shaking table tests. In a uniaxial shaking table exposed to sinusoidal base excitation, a laminar box was mounted in which the geogrid reinforced reduced scale models of retaining wall were constructed. Effects of reinforcement type, backfill density on the performance of small scaled modelled

retaining wall were evaluated through a series of laboratory tests. Performance of walls was evaluated in terms of crest settlement, face deformations on the backfill side facing of the wall and acceleration amplification computed at different heights of the retaining walls and compared.

A self-designed and built laminar box was used for the assembly of shaking table to reduce the end effects on model structures to the least by minimizing the friction. Locally available dry sand of grade SP was used in this study. A special technique known as sand pluviation was used in placing the sand in the laminar box for the achievement of uniform density of the backfill soil.

In both the cases of rigid and modular retaining walls, the lateral displacement of retaining wall increased with the height of the wall from the base of the shaking table during base shaking. As the backfill density was increased, the deformation in the wall reduced both in case of rigid and modular wall, the outcome was highly distinct in case of modular block wall. At any particular height, the rigid faced wall faced fewer deformations than modular block walls. The reinforcements had a more pronounced effect on the modular block wall in case of reducing deformations. Acceleration amplification was more in situation of reinforced wall in comparison to unreinforced wall and the acceleration amplification was distributed non-uniformly with the height of the wall from the base of the shake table. The quantity of reinforcement used was inversely proportional to the settlements for all the tests. The perpendicular deformations were decreased by about 60% in both the used walls when three levels of reinforcement were placed in the backfill soil while carrying out the tests.

Tabaroei Abdolah, Abrishami Saeed and Hosseininia Ehsan Seyedi (2017), conducted a study for the provision of constant reconstituted sand specimens of desired density. In this

study, for the preparation of homogeneous sand specimen, two sand raining techniques were introduced, i.e. a perforated plate raining system and a portable curtain raining system. The effects of height to fall and deposition intensity on the R.D. of reconstructed sand specimens were studied and a better understanding of them was provided in this study.

Only portable curtain raining system was noted to be capable in preparing a wide range of relative densities i.e. between 23.2% - 95.8%. By using the method of perforated plate, a limited range of relative densities were achieved i.e. between 32.9% - 73.7%.The relative density of the reconstituted soil specimen enhanced with the enhancement in height of fall in both the cases, the effect of height of fall on relative density was more pronounced at lower heights as compared to when height of fall was more. With the increasing deposition intensity, the R.D. of the reconstituted soil specimen decreased. The highly dense and normally dense sand specimens were obtained by regulating the deposition intensity. The homogeneity of the reconstituted soil specimens also improved by using both the techniques for any relative density.

2.2 Summary

S.No.	Author Name	Year of Publication	Type of Retaining Wall	Experimental Setup (Centrifuge or Shake Table)	Base Acceleration Range (g)	Frequency Range (Hz)	Amplification Ratio (Acceleration Top/Acceleration Bottom)
1.	G. Madhavi Latha, A. Murali Krishna	2008	i. Wooden Plank Wall	Shake Table	i. 0.1 ii. 0.2	i. 1 ii. 2-5	i. 0.99 – 1.06 ii. 1.71 – 1.91
2.	G. Madhavi Latha, P. Santhanakumar	2015	i. Rigid Faced Steel Walls ii. Modular Block Concrete Wall	Shake Table	i. 0.3	i. 2	i. 1 – 1.25 ii. 1 – 1.28
3.	Liyan Wang, Guoxing Chen, Su Chen	2015	i. Rigid Faced Concrete Wall	Shake Table	i. 0.05 – 0.5	i. 0 – 25	i. 0.5 – 2.4
4.	Roozbeh Geraili Mikola et al.	2015	i. Stiff Braced Wall ii. Flexible Braced	Centrifuge	i. 0.02 – 0.69	-	-

5.	M. M. El-Emam, Richard J. Bathurst	2006	i. Rigid Panel Steel Wall	Shake Table	i. 0.05 – 0.6	i. 5	i. 1 – 2.8
6.	A. Komak Panah et al.	2015	i. Concrete Panel Wall	Shake Table	i. 0.2 – 0.85	i. 4.53	i. 0.9 – 1.7
7.	A. L. Simonelli et al.	1998	i. Concrete Gravity Wall	Shake Table	i. 0.175 – 0.411	i. 5	-
8.	R. Conti et al.	2012	i. Aluminium Alloy Wall	Centrifuge	i. 0.05 - 0.41	i. 1 – 1.5	-
9.	Robb Eric S. Moss et al.	2012	i. Flexible Wall Barrel	Shake Table	i. 1.5	i. 0.316	-
10.	Erol Guler and Ali K. Enunlu	2009	i. Concrete Panel Wall	Shake Table	i. 0.23	i. 3	1.21 – 1.9
11.	Luciano Oldecop et al.	1996	i. Steel Gravity Wall	Shake Table	i. 0.25 - 1	i. 10	-

CHAPTER 3
METHODOLOGY

3.1 Introduction

Assessment of dynamic response of retaining wall is one of the prominent considerations before construction of any such structure. The response is affected by factors such as backfill density, surcharge, interface friction between wall and soil, base excitation, inclination of backfill. Ascertaining the factors that most influence the response, govern the design criterion. Numerous experimental tests and numerical investigations have been attempted to understand the governing parameters.

Most of the experimental investigations are carried out by constructing a reduced scale retaining wall on shaking table and measuring response by varying different parameters. In present study, the response of soil retaining wall small scale models structured at different backfill R.D. and subjected to different levels of base acceleration excitation is evaluated in terms of linear static and dynamic displacements of the facing wall and accelerations in backfill at top level of facing.

The inputs, outputs and the experiments performed for the study along with the path followed for the study are shown in the form of a flow chart is shown in the Figure 3.1 in the following page.

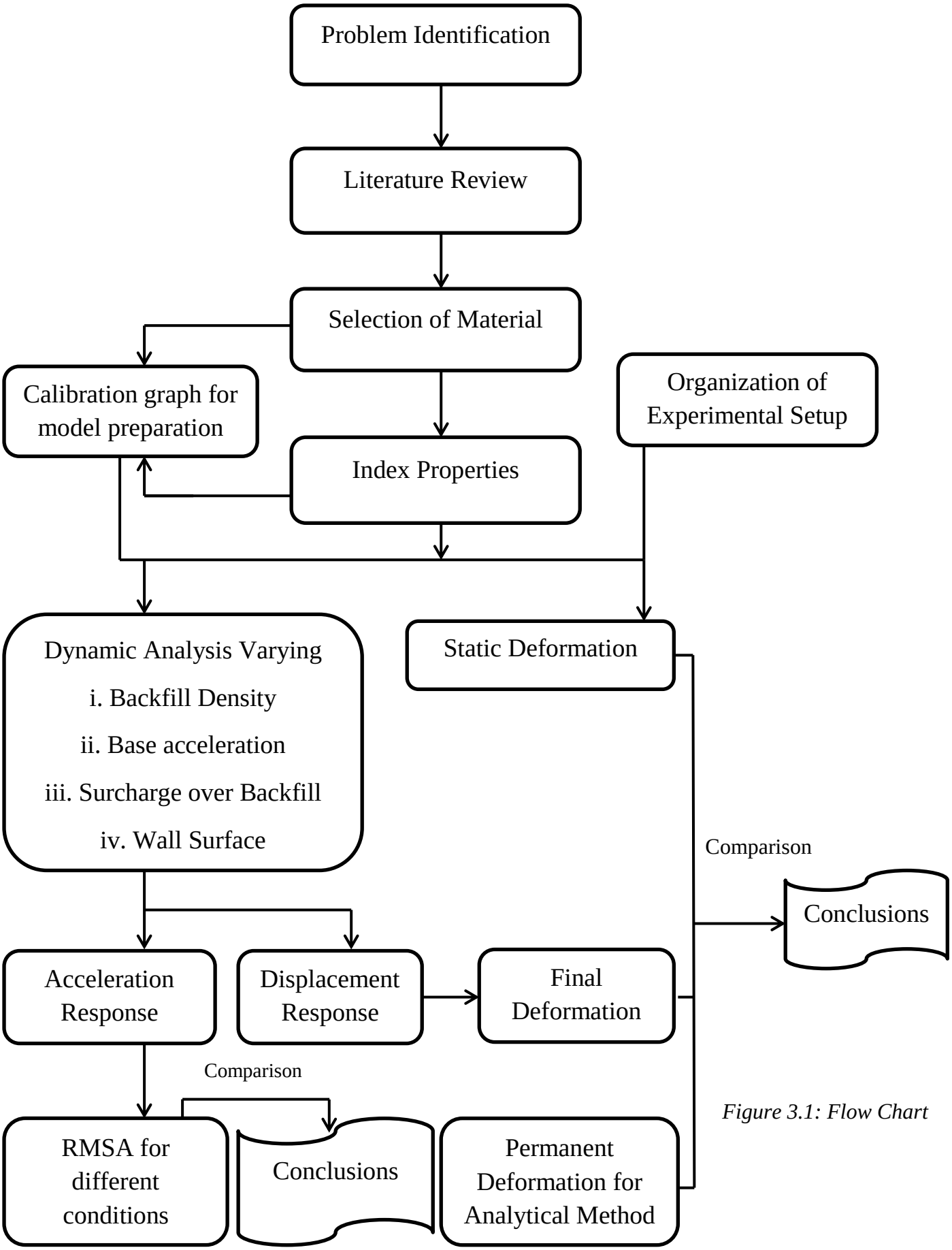

Figure 3.1: Flow Chart

3.2 Materials used in Experiment

3.2.1 Backfill Material

The soil which the retaining wall holds back and retains is the backfill of the retaining wall. A retaining wall should preferably have well compacted backfill. The backfill material should be selected such that it can be easily compacted and possess sufficiently high permeability to not allow pore water pressures to build up. Hence, coarse soil is most suitable to be utilized as backfill material for retaining walls subjected to their availability.

Dry uniformly graded sand is used as the backfill material. The Grain size analysis of the soil is done in accordance with the IS 2720 Part 4: Grain size analysis. In Figure 3.2, the grain size distribution of the backfill material can be seen. The sand used for backfilling is categorized as poorly graded sand with letter symbol SP as per the Indian Soil Classification System.

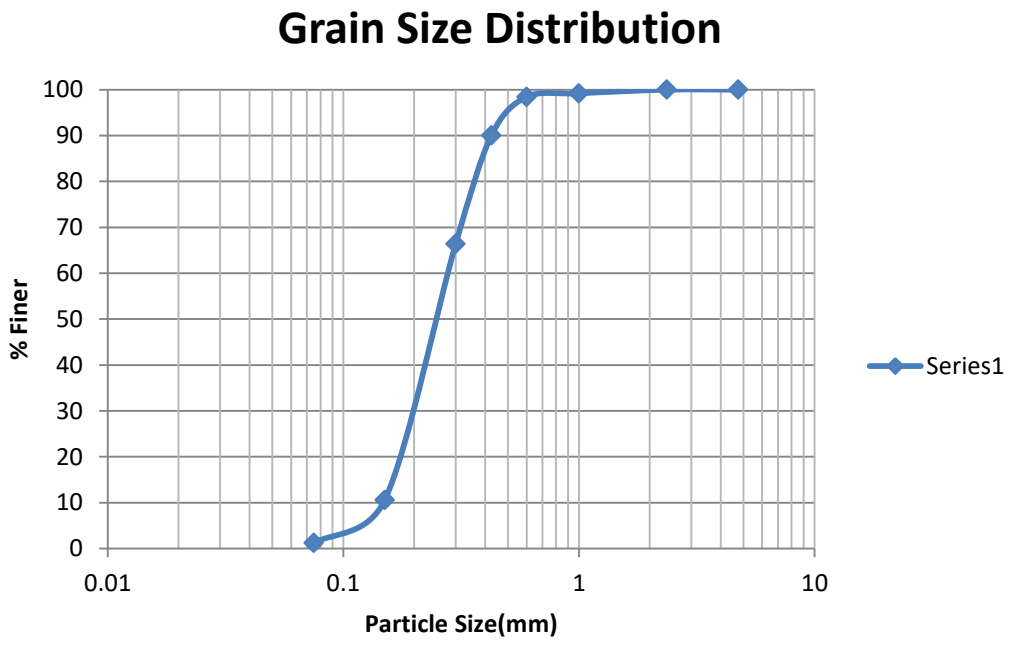

Figure 3.2: Grain Size Distribution

From the graph, we can see that about 62 % of the soil size lies in between 0.1 mm to 0.3 mm. D10, D30 and D60 of the soil are also calculated from the graph using interpolation. The maximum and maximum unit weight are also calculated which come out to be 18.394 kN/m³ and 13.475 kN/m³ respectively. The coefficient of Curvature (Cc) and coefficient of Uniformity (Cu) are calculated and equal to 0.997 and 1.944 respectively. From these properties, we can conclude that the soil is of grade SP.

Different index properties of the backfill soil are also calculated by performing laboratory experiments. The density variations in the backfill sand are obtained by performing density determination tests on backfill sand in both the dry and wet state. This test is done in accordance with the IS 2720 Part 14: Determination of density index (relative density) of cohesion less soils. Specific Gravity of the sand is found using Pycnometer Apparatus according to IS 2720 Part 3: Determination of specific gravity, Section 2: Fine, medium and coarse grained soils. The other index properties are also determined and are shown in Table 3.1.

Table 3.1: Index properties of test sand.

Specific Gravity	2.67
e_{max}	0.727
e_{min}	0.532
D-10(mm)	0.145 mm
D-30(mm)	0.202 mm
D-60(mm)	0.282 mm
Coefficient of Curvature(Cc)	0.997
Coefficient of Uniformity(Cu)	1.944
Maximum Dry Density	1.877 gm/cc

Minimum Dry Density	1.375 gm/cc
Maximum Wet Density	2.275 gm/cc
Minimum Wet Density	1.77 gm/cc
Maximum Unit Weight	18.394 kN/m³
Minimum Unit Weight	13.475 kN/m³
Soil Classification as per USC system	SP

Direct shear test is also conducted on the backfill soil used in the study. The maximum shear stress capability of the soil and the angle of internal friction of the soil are determined by this test. The Normal Stress – Shear Stress plots are also obtained from the direct shear test. They have been conducted on dry sand samples at three different relative densities of 35%, 45% and 55%. The corresponding internal friction angles are calculated as 33.51°, 36.09° and 38.18° respectively. The Normal Stress – Shear Stress plot corresponding to R.D. 35%, 45% and 55% is shown in Figure 3.3. The direct shear test is done according to the IS 2720 Part 13: Direct shear test.

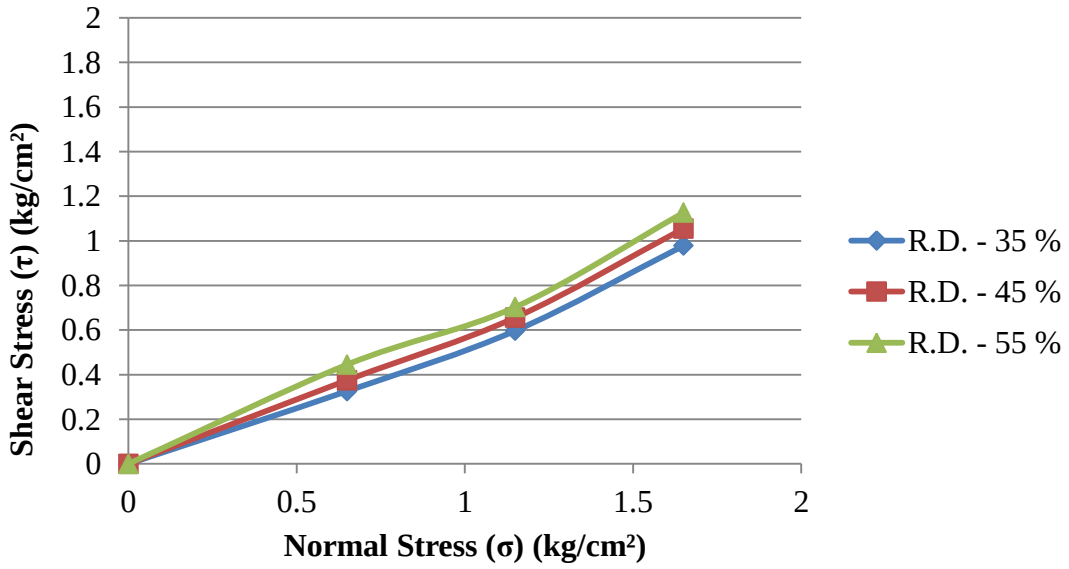

Figure 3.3: Direct shear test result (R.D. = 35%, 45% and 55%)

From the graphs in the Figure 3.3 we can clearly see that with the increasing relative density of the soil, the angle of internal friction (Φ) of soil also increases. Increasing the relative density from 35% to 45% to 55% result in rise in angle of internal friction from 33.51° to 36.09° to 38.18° respectively. This happens due to increasing packing of particles with the rise in the density of soil. From the angle of internal friction of soil, it is also concluded that soil is sand.

3.2.2 Retaining Wall

A structure which can hold or retain soil behind it is known as a retaining wall. Retaining walls can be constructed from numerous different materials such as timbers, and rocks, poured concrete and concrete blocks. Each one of these material has its own pros and cons but all can retain the earth behind them.

Nowadays, concrete block retaining walls are becoming increasingly popular due to their high strength and high durability. Gabion retaining walls are still made in some areas where their availability is easy. Timber retaining walls are used is areas where the pressure on the walls is less or in small scale construction. (A.M. Goncalves et al., 2018).

For the present study, different thicknesses of dry oak red wood are used for small scale model of retaining wall. Three different types of wall are used:

1. 24 mm thick single wall panel of size 585 mm by 400 mm. The top of wall deformations are very small for even very high levels of acceleration, hence thinner section is used for further study.
2. To achieve exaggerated deformations, a thinner rough wall section of 12 mm thickness is used for further parametric study. These panels are connected to each other after backfilling each panel by two vertical strips of thickness 12 mm and size 30 mm * 12.7 mm. This wall is shown in the Figure 3.4. A three panelled wall is chosen to

resemble the sequential construction of an actual retaining wall. Firstly, the base panel is attached and then after sand raining the 2nd and in same manner the 3rd panel.

Figure 3.4: 12 mm thick 3 panelled staged wall.

3. 12 mm thick three panel reduced friction wall of the same dimensions as that of wall in Figure 3.4 is also used. To reduce friction, sunmica is affixed on the panels of the rough wall using wood adhesive. Sunmica is a blend of paper and plastic. It is a smooth laminated sheet which considerably reduces the surface friction. This wall is as shown in the adjoining Figure 3.5.

Figure 3.5:12 mm thick 3 panelled reduced friction wall.

3.2.3 Sensors

3.2.3.1 Linear Variable Differential Transformer (LVDT)

LVDT is a type of electric transformer utilized for computing displacement and linear position. For the research purpose, two AG Measurematics Alternating Current LVDT's are used. These LVDT's have a range of ± 25 mm. Both the forward and backward displacement can be measured using these LVDT's. The dynamic and static linear displacement of the retaining wall is measured using these LVDT's. Displacement is measured at the top and at the middle of the wall. Static displacement is measured after the sand raining upon reaching the desired density of the soil but before the application of sinusoidal motion on the wall. Dynamic linear displacement is measured after the application of sinusoidal motion on the retaining wall. Both the LVDT's used are shown in the adjoining Figure 3.6.

Figure 3.6: AG Measurematics Alternating Current LVDT.

A heico data logger is also used for the present study. It is used for computing static and dynamic linear displacement of the wall before and after the application of sinusoidal

motion on the wall respectively. LVDT's are connected to the data logger and are placed at the top and middle of the wall. The data logger has built in software for the computation of data over a period of time. The heico data logger has a limitation as it is only able to record data at a minimum time interval of 0.5 seconds.

3.2.3.2 Accelerometer

An electromagnetic device mainly used in measuring acceleration forces is known as an accelerometer. Acceleration forces may be dynamic or static. Earthquakes can also be detected using motion sensors in accelerometers. The accelerometer used for the present study is Micron Optics accelerometer model os7100 which is a fibre optic accelerometer based on FBG (Fibre Bragg Grating) technology. It is available in up to three axis configurations. It has a rugged sealed metal body and is waterproof for usage in hard outdoor conditions. Micron Optics os7100 can be seen in Figure 3.7. For the present study, os7100 is used to measure dynamic acceleration of the sinusoidal motion applied on the retaining wall by the shaking table at top and at the bottom. Accelerometer is affixed at the base of the shaking table for base excitation and is embedded within the soil at a distance of 10 cm from the wall for measuring the top excitation.

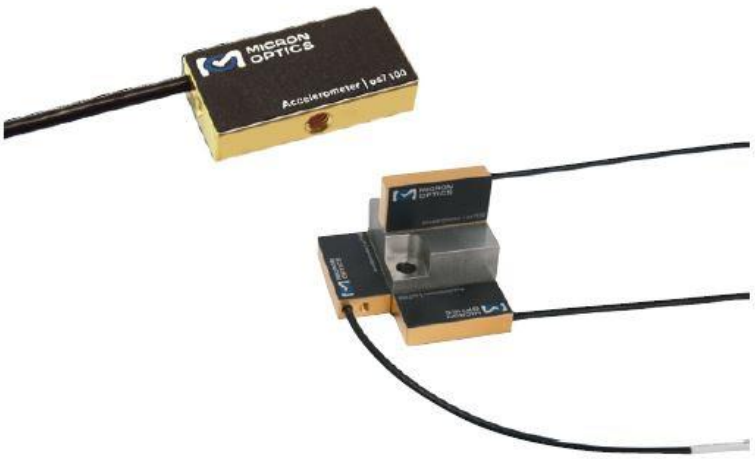

Figure 3.7: Micron Optics Accelerometer os7100.

A micron optics static optical sensing interrogator model sm125 is also used. It has 4 optical channels with a scan frequency of 2 Hz. It has a wavelength range of 1510 – 1590 nm. For the present study, accelerometer sensor os7100 is connected to the sm125 optical interrogator which was in turn connected to a computer using an Ethernet cable. This gives the acceleration readings at the top and bottom of the shaking table at regular intervals of 0.1 seconds.

3.3 Equipment Setup

3.3.1 Shaking Table

Since the sixties, using shaking table has been an effective way for the measurement of dynamic performance of small scale structures. A considerable amount of research has already been carried out on shaking tables and it can be easily found in the literatures. Bairrao and T Vaz (2000) presented some attributes of the latest experience attained through the execution of numerous series of tests on different type of assemblies which were executed using a LNEC 3D earthquake simulator.

It has become possible to decipher the dynamic performance of the specimen with the help of data from transducers, data loggers and video records. With the help of shaking tables, we can excite the structures in such a way that it resembles the real earthquake ground motions.

For the present research, a mechanically controlled single degree of freedom shaking table facility is used for assessing the seismic and dynamic behaviour on different retaining wall models. The shaking table includes an enclosed area of size 990 mm * 584 mm * 584 mm. The shake table is a single axis; electrically controlled and has provision for changing the base acceleration. The maximum displacement amplitude applied for the

present research work is 2.5 mm. The shaking table assembly is as shown in adjoining Figure 3.8.

Figure 3.8: Shake Table assembly.

3.3.2 Metal Frame

A custom metal frame is made with a rectangular section open from one end where supports are provided for it to stand still. The rectangular section is made using the hollow iron pipes. A two inch angular section is fixed at the centre of the metal frame from the top. The height of the frame is made to be 2 metres to ensure the maximum height during the height of fall. The width of metal frame is made to be 0.8 metres which is greater than the width of the shaking table assembly. This is done to ensure that the sinusoidal motion applied by the shaking table does not affect the movement of the frame.

The metal frame does not have any contact or connection with the shaking table and isn't affected by the movement of shaking table when the sinusoidal motion is applied. To

ensure this, weights are kept on the supports of the frame while the experiments are conducted.

The main purpose of the metal frame is to hold the affixed LVDT's in their place so that the linear displacement of the retaining walls could be measured. To ensure this, holes are provided on the angular section of the frame where the LVDT's are fixed using nuts and bolts at the required height i.e. at the middle and top of the retaining wall. The metal frame is also provided with markings for different heights from 1 metre to 2 metre for the purpose of ensuring the height of fall for sand pluviation. Metal frame placed inside the shaking in the position of recording displacement is shown in Figure 3.9.

Figure 3.9: Metal Frame.

3.3.3 Sand Raining Sieve

A custom sieve is made of size 1.75 mm for the process of sand raining. The sieve is enclosed in a wooden frame of size 900 mm * 500 mm. It is held at different heights above the shaking table with the help of the markings on the metal frame and the sand is made to fall uniformly over the sieve and thereby into the shaking table. Changing the height of the sieve results in the variation in the density of the backfill soil. The custom made sieve is as shown in Figure 3.10. A thin plastic sheet is affixed at the ends of the wooden frame to prevent the wastage of sand as sand can be blown away when raining is carried out.

Figure 3.10: Custom made sieve of size 1.75 mm.

To attain the required density of backfill, sand raining (pluviation) technique is used. In this technique, sand is poured from this custom made sieve from a certain height to achieve the desired density. For achieving the desired density, sand is poured uniformly

over the sieve through with it falls uniformly in the shake table. As specified by Tabaroei et al. (2017), the R.D. of the reconstituted soil specimen increases with the increase in the height of fall. For obtaining highly dense specimens, the deposition intensity needs to be decreased.

The density of the sand varies with variation in the height of fall. To determine the height of fall for achieving different densities of backfill, a series of trials are performed with different height of fall using a mould of known volume. These series of trials are tabulated and the height of fall required for different relative densities is computed.

For the trails and formulation of calibration chart, a mould of volume 1000 cc is used. Sand is poured from the height ranging from 1.6 m to 2.0 m. Numerous trials are conducted for every height and the density achieved corresponding to height of fall is formulated.

The different densities achieved changing the height of fall are graphically plotted and shown in Figure 3.11.

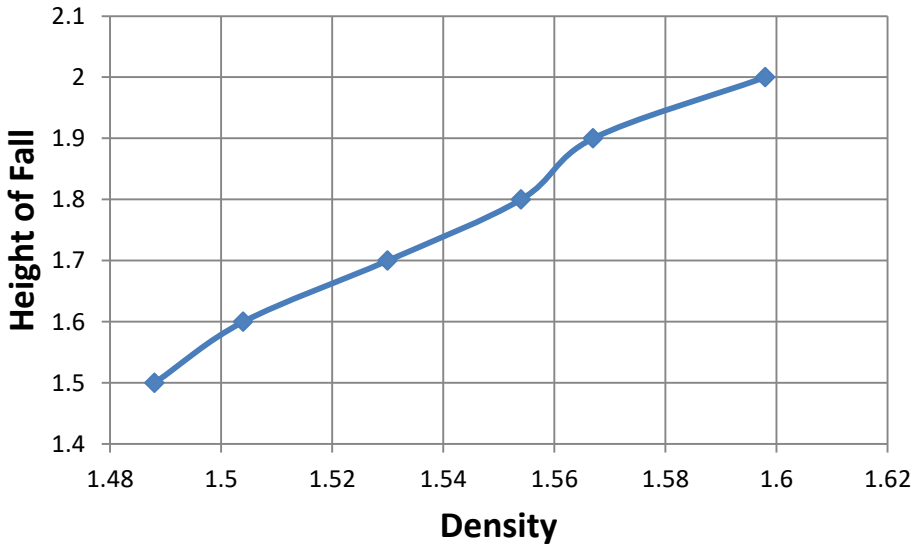

Figure 3.11: Calibration Graph for Sand Pluviation.

For the study, soil had a maximum density of 1.877 gm/cc. Tests are carried out at a relative density of 35%, 45% and 55%. The densities corresponding to these relative densities are 1.5 gm/cc, 1.55 gm/cc and 1.6 gm/cc respectively.

To achieve these densities, sand pluviation technique is used. The height of fall for sand pluviation is determined by the calibration chart. From the graph shown in Figure 3.11, we can see that the densities 1.5, 1.55 and 1.6 gm/cc are achieved by keeping the height of fall of sand at 1.6 m, 1.8 m and 2.0 m respectively.

3.4 Model Construction

In the study, small scale model of retaining wall is constructed in the shaking table of size 1000 mm * 590 mm in plan and 590 mm deep. Keeping in mind the proportions, the retaining walls are made 400 mm in height and are kept 600 mm from the backfill side of the shaking table. Sand is used in backfilling all the model walls and are constructed in equal lifts as mentioned earlier. All studies are done using rigid facing. Static deformation are measured at top and mid of wall using LVDTs. After that, sinusoidal motion is applied on the small scale model of retaining wall by the shaking table and the acceleration data is recorded at top and bottom to measure amplification under different conditions. Lateral deformation is measured at the top and mid of retaining wall facing simultaneously.

Schematics of characteristic model configurations beside the layout of the instrumentation for the test model walls are shown in Figure 3.12 for different wall models. Accelerometers A1 and A2 are embedded in the soil and LVDT's L1 and L2 are attached to a custom metal frame on the opposite side of the backfill. To compare the results, the accelerometers and LVDT's are placed in the identical locations in all the tests.

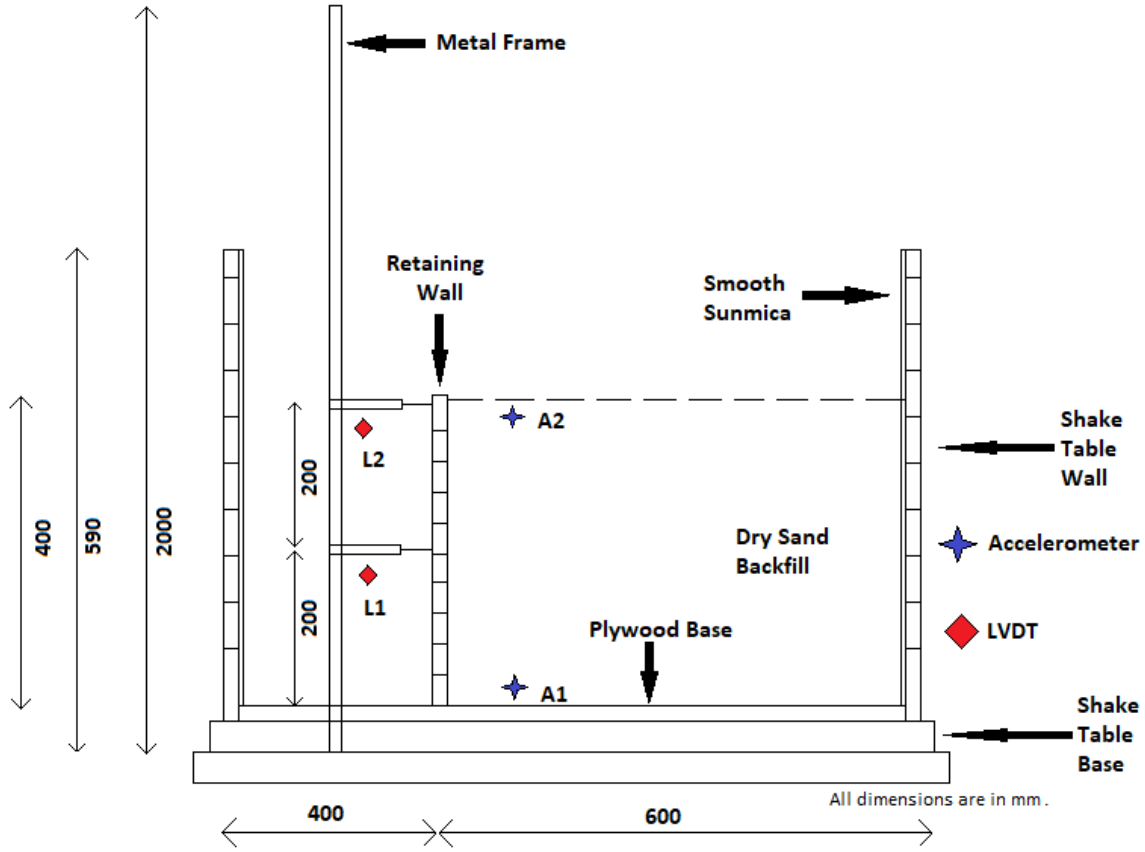

Figure 3.12: Schematic of the Shaking Table Model Assembly.

Various steps are followed in the construction of the small scale model for the retaining wall. These steps are as follows:

Firstly, to make the walls of the shaking table with minimum friction so that they do not have any effect on the free motion of backfill during the application of sinusoidal motion, the walls of the shaking table are covered with reduced friction surface of sunmica. Sunmica is affixed on the three sides of the shaking table where the backfill is supposed to be filled. The affixed sunmica can be seen as shown in the Figure 3.13.

Figure 3.13: Sunmica Affixed to the Walls of Shake Table.

To provide a fixed bottom condition of the retaining walls, the base of the shaking table is made of plywood. 24 mm thick plywood of size 990 mm * 585 mm is affixed at the bottom of the shaking table before the setting up of retaining wall. The plywood base is as shown in the adjoining Figure 3.14.

Figure 3.14: Plywood Base of the Shaking Table.

Then for fixing the 1st wall i.e. single panelled wall of thickness 20 mm and dimension 585 mm * 400 mm, this wall is fixed with the plywood at the base using three aluminium angles on each side and screws.

In case of staged wall of thickness 12 mm, the facing of the wall is constructed using three panels of width 585 mm and height 117 mm, 166 mm and 117 mm respectively starting from the bottom. These panels are joined together using two vertical wooden columns. Firstly, the bottom panel is affixed with the plywood base (including the two vertical wooden columns) in the same manner as earlier walls. Then after the backfill is introduced to the first panel, the next panel is fixed using the vertical wooden columns and screws and same procedure is followed until the sand raining is completed.

In case of staged friction less wall, the facing of the staged wall is affixed with sunmica. All the three panels of the staged wall are affixed with low friction sunmica using adhesive. After fixation, same steps are followed as in case of staged rough wall to carry out experiments and recording data.

In case of experiments for surcharge, staged panel rough wall is used. After completing the pluviation with the setting up of all the panels, a surcharge of 2 kg is kept at the centre of the backfill i.e. at 300 mm from the retaining wall and 295 mm from the wall of the shaking table. The rest of the experimental procedure is followed as same.

After affixing the retaining wall with the plywood base of the shaking table, LVDT's are fixed with the metal frame and placed adjoining the retaining wall on the opposite side of where the backfill is to be filled. Two LVDT's are placed, one at the top of the wall and other at the middle of the wall. In case of staged wall, the LVDT which is to be placed at the middle is attached after affixing the 2nd panel and the LVDT which is to be placed at

the top is attached after affixing the 3rd panel. The attached LVDT's to the metal frame are as shown in Figure 3.15.

The LVDT's are such that there is considerable space between the LVDT end and the wall of the shaking table. This is done to ensure that hindrance by the shaking table wall does not affect the recording of displacement data.

Figure 3.15: Attached LVDT's to the metal frame.

After this, backfill is introduced to the retaining wall. To attain uniform density throughout, sand is poured in the shaking table using the pluviation (raining) technique. Using this practise, the sand is made to free fall through a custom made sieve of size 1.75 mm from different heights according to required densities. The sand passes through the cross section of the sieve and disperses at the bottom. A sequence of trials is performed at different heights to ensure the height of fall of sand to attain the desired density of the backfill. While pouring, same height is maintained throughout to achieve the desired density.

The experimental plan is formulated such as to examine the effect of relative density of backfill soil on the dynamic and static response of the soil retaining wall models with varying sinusoidal motions applied by the shaking table at different acceleration amplitudes.

For recording the dynamic response of the wall model at varying relative densities and different acceleration amplitudes, accelerometers were located at the bottom of the shaking table i.e. at the plywood base and also embedded in the backfill soil at the top of the soil about 10 cm away from the retaining wall model.

3.5 Similitude Laws

In the present study, the tests are done on small scale models of prototype retaining walls. Due to less restraining pressures and end effects in the study of the model, the deformation and stress measurements in the tests do not accurately exemplify the stresses and distortions in the real conditions. To minimize this difference and in order to apply the results to real conditions in the world, it is necessary to make use of proper similitude laws for the experiment. Similitude laws were presented by Iai (1989) from the fundamental definition of strain, stress, overall equilibrium for 1 g model tests. This was done in between the real conditions and model using prototype geometry, a geometric scale factor λ, was expressed as the proportionality constant. For other parameters also, similar proportionality equations were assumed.

Because of the gravity and scaling effects, it is not possible to straightforwardly extrapolate the results from these model tests to get the reaction of field walls, the results acquired from this study are beneficial in identifying the relative performance of rough, reduced friction and rough with surcharge soil retaining walls with different backfill R.D. exposed to changing shaking levels.

For the present study, the geometric scale factor λ is taken as 12. According to this, the height of the model wall is kept at 0.4 m, corresponding to 4.8 m in the field. The scaling factors computed for relating various physical quantities in models to those in the prototype are given in Table 3.2.

Table 3.2: Similitude laws for shaking table model test

Parameter	**Model Parameter**	**Equation for scaling (Prototype/Model)**	**Scaling Factor**	**Prototype Parameter**
Acceleration (g)	i. 1.441 ii. 0.843 iii. 0.776	1	1	i. 1.441 ii. 0.843 iii. 0.776
Unit weight of sand (kN/m³)	i. 15.68 (55% R.D.) ii. 15.19 (45% R.D.) iii. 14.7 (35% R.D.)	1	1	i. 15.68 (55% R.D.) ii. 15.19 (45% R.D.) iii. 14.7 (35% R.D.)
Dimensions of wall (B*H) (m)	0.585 x 0.400	λ	12	7 x 4.8
Frequency (Hz)	i. 0.779 ii. 0.795 iii. 0.806	$1/\lambda^{3/4}$	0.155	i. 0.120 ii. 0.123 iii. 0.125
Time	t_m	$\lambda^{3/4}$	6.45	6.45 x t_m
Stress	σ_m	λ	12	12 x σ_m

3.6 Root Mean Square Acceleration (a_{rms})

Parameters such as Kanai–Tajimi, shape factor etc. which are primarily related to the amplitude of the vibration, frequency of the vibration, or duration of a ground motion. As all of these features are vital, ground motion parameters which imitate more than one of these characteristics are very beneficial. The rms acceleration is one of such parameter which incorporates the effect of both amplitude and frequency content of a strong motion. (Kramer, 1996). The rms acceleration value is defined as shown in equation 1.

$$a_{rms} = \sqrt{\frac{1}{T_d}\int_0^{T_d}[a(t)]^2 dt} = \sqrt{\lambda_0} \quad \text{.....equation 1.}$$

where, T_d is the duration of the strong motion and λ_0 is the average intensity (or mean-squared acceleration). The integral equation 1 is not strongly influenced by large, high-frequency accelerations (which occur only over a short period of time) but it is influenced by the duration of the motion. Due to this, the rms acceleration can be very useful for engineering objectives and applications. So, for the present study the rms acceleration values are used for computing acceleration amplification. RMSA amplification factor is the ratio of RMS acceleration record value in the soil to the corresponding base RMS acceleration value.

3.7 Displacement by Whitman & Liao (1980) Method

To validate the dynamic displacement data records taken by LVDT's the theoretical maximum displacement due to the application of sinusoidal motion at varying accelerations is calculated using the method given by Whitman & Liao (1980). Theoretical maximum displacement is calculated corresponding to the three panelled rough wall.

Whitman and Liao (1980) used the results of a sliding block analysis of 14 ground motions carried out by Wong (1982), and obtained the permanent displacements using lognormal distribution with mean value as shown in equation 2.

$$\bar{d}_{perm} = \frac{37\, v_{max}^2}{a_{max}} \exp\left(\frac{-9.4\, a_y}{a_{max}}\right) \quad \text{.....equation 2.}$$

The maximum value of velocity (v_{max}) is assumed at different accelerations and relative densities. The maximum value of acceleration (a_{max}) is recorded for different acceleration amplitudes using accelerometer. The yield acceleration a_y is given by relation given by Whitman and Liao (1985) i.e. $a_y/a_{max} \geq 0.4$.

CHAPTER 4
RESULTS AND DISCUSSION

4.1 Introduction

In this chapter, the detailed results of tests performed on small scale model of retaining wall at different backfill density, base acceleration, wall surface and surcharge are given.

Initially, in the first section dynamic and static responses of the rough retaining wall with respect to various parameters, backfill density, base acceleration intensity, surcharge and wall surface is presented. The Root Mean Square Acceleration (RMSA) comparison for different acceleration and relative density is also presented and discussed. At last, theoretical displacement at different accelerations using Whitman and Liao (1980) approach is calculated and produced.

4.2 Response of rough wall

In this section, the results corresponding to effect of various parameters on static and dynamic response of rough retaining wall is presented. Variation of acceleration with depth is presented in terms of RMSA for each combination.

4.2.1 Effect of backfill density

In the present study, both the static displacement i.e. displacement of the walls before the application of sinusoidal motion and dynamic displacement i.e. displacement of the walls after the application of sinusoidal motion are recorded using the LVDT's. Both the dynamic and static displacement is recorded at three varying amplitudes of sinusoidal motion. Displacement is recorded at two points, at the top of the wall and at the middle of the wall i.e. at 400 mm and 200 mm from the bottom of the shaking table respectively.

For acceleration 1, the maximum amplitude of acceleration is recorded as 1.441 g. This sinusoidal motion is applied to the small scale model of retaining wall and backfill density at varying relative density of 35%, 45% and 55%. The lateral displacement before the application of sinusoidal motion i.e. static displacement and after the application of sinusoidal motion is recorded and shown in Figure 4.1. Comparisons are made between the lateral displacements at varying relative densities at this acceleration.

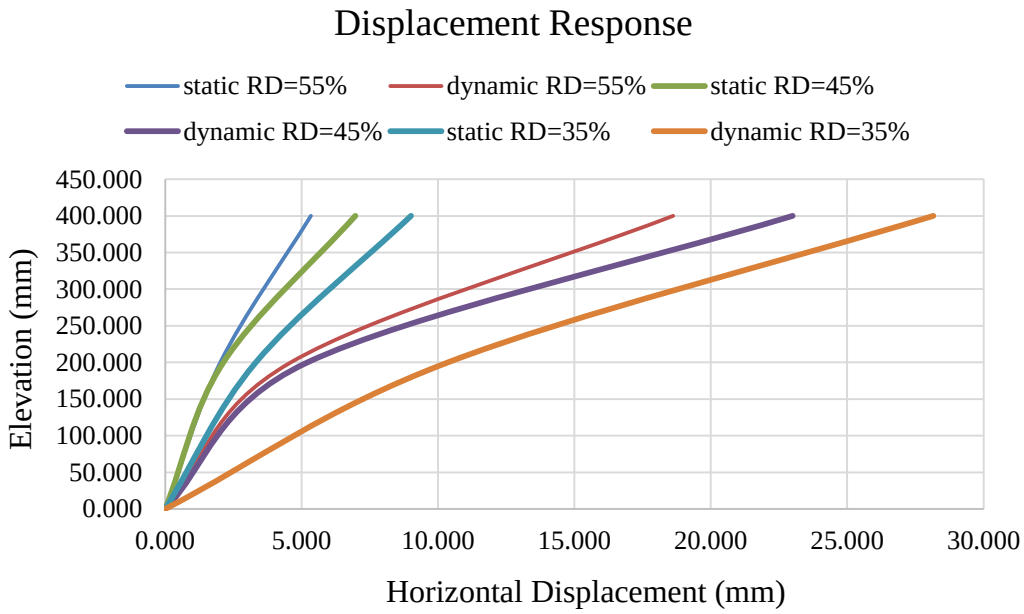

Figure 4.1: Displacement Response at base acceleration level 1.

From the graph, we can see that static displacements are about 200% less than dynamic displacements of the retaining walls which are recorded after the sinusoidal motion are applied. The maximum static and dynamic displacements are recorded at the top of the wall. Observing the change in lateral displacements with respect to the relative density of the backfill, it is observed that both the lateral static and dynamic displacement decrease with an increasing relative density of the backfill.

For the acceleration 2, the maximum amplitude of acceleration applied by the shaking table is recorded as 0.843 g. For this acceleration also, lateral static and dynamic displacements are recorded at relative densities of 35%, 45% and 55%. The results are graphically formulated and shown in Figure 4.2. Comparisons of lateral displacement are made at different relative densities as shown in the figure.

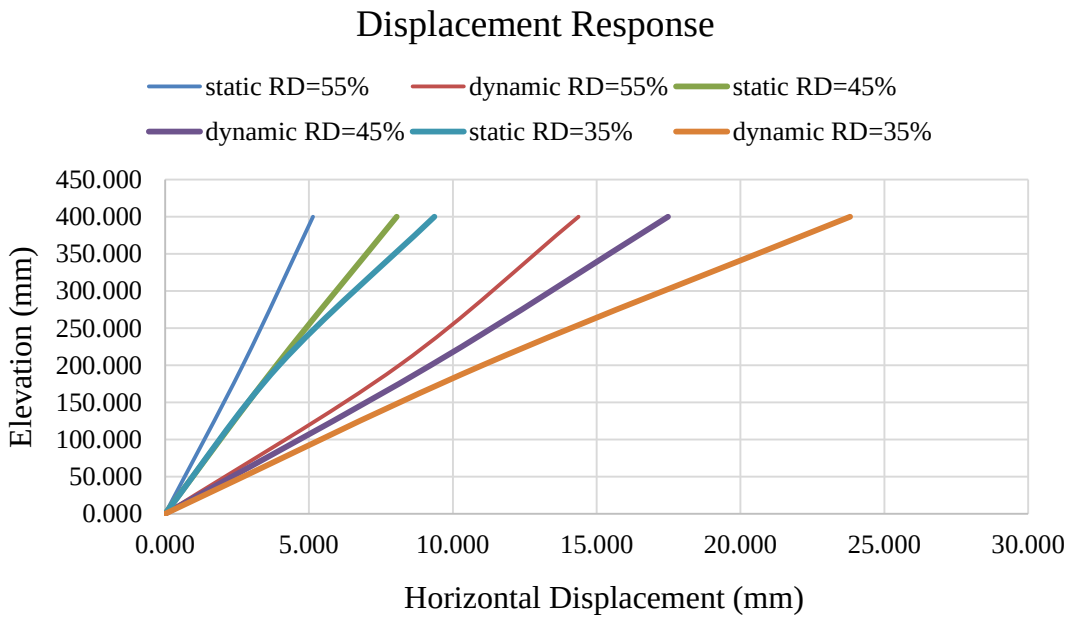

Figure 4.2: Displacement Response at base acceleration level 2.

From the graph, it is seen that same pattern of displacement is followed as in previous acceleration amplitudes i.e. the static displacements are about 150 %less than the dynamic displacements. The lateral displacements tend to decrease with an increasing R.D. of the backfill. The maximum displacement occurs at the top of the retaining wall.

For the acceleration 3, the maximum acceleration amplitude is recorded equal to 0.776 g. Top and bottom displacements of retaining wall are detailed at this acceleration corresponding to different relative densities. The result corresponding to this acceleration

showing the lateral displacement at the top and mid of the wall are shown in the adjoining Figure 4.3.

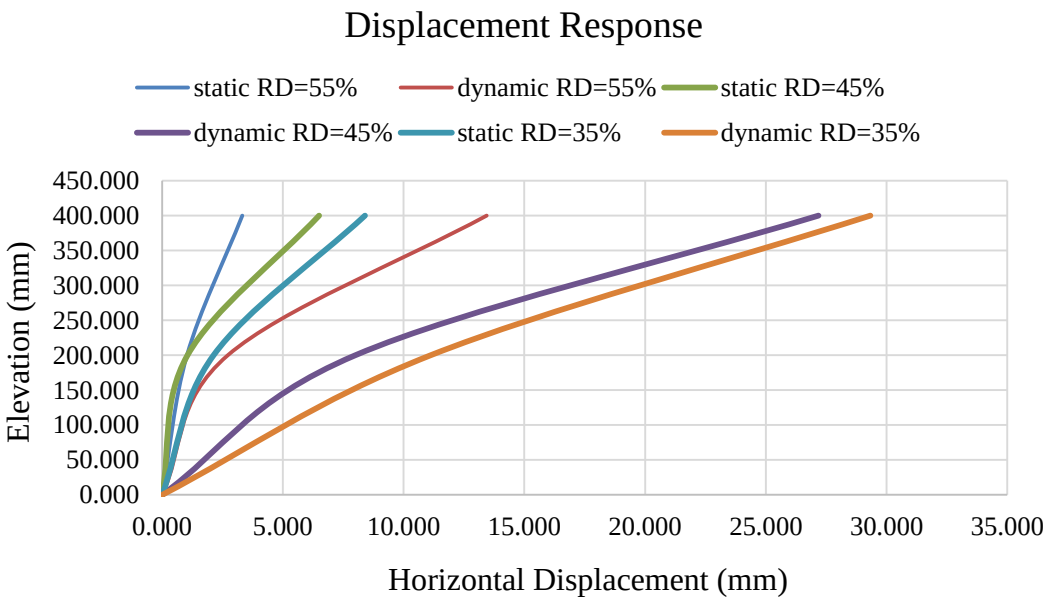

Figure 4.3: Displacement Response at base acceleration level 3.

From the graph it can be clearly seen that between static displacements of relative density 55% and 45%, the displacement at the mid of the retaining wall in the case of relative density 45% is slightly greater than 55% relative density whereas rest of the static displacement follows the same pattern as in case of earlier accelerations. The dynamic displacement also follows the same pattern as earlier as it decreases with the increase in relative density of backfill. Dynamic displacements are about 300 % more than static in this case.

In this section, the acceleration response variation corresponding to rough wall at the top of the backfill at varying relative densities is also presented. The accelerometer is placed at the top of the backfill 10 cm from the facing of the wall. At the base, three acceleration amplitudes are recorded at which the tests are performed for different relative densities. The acceleration response at the top is recorded corresponding to each backfill density

and varying base acceleration. The acceleration response recorded at the top for rough wall at varying backfill relative density is produced and described in this section.

For acceleration 1, the maximum amplitude of base acceleration is 1.441 g. At this amplitude of base acceleration, acceleration response at the top of backfill is recorded at relative densities of 35%, 45% and 55%. The top acceleration response corresponding to this acceleration at relative density of 55% and 35% is as shown in Figure 4.4 and Figure 4.5 respectively.

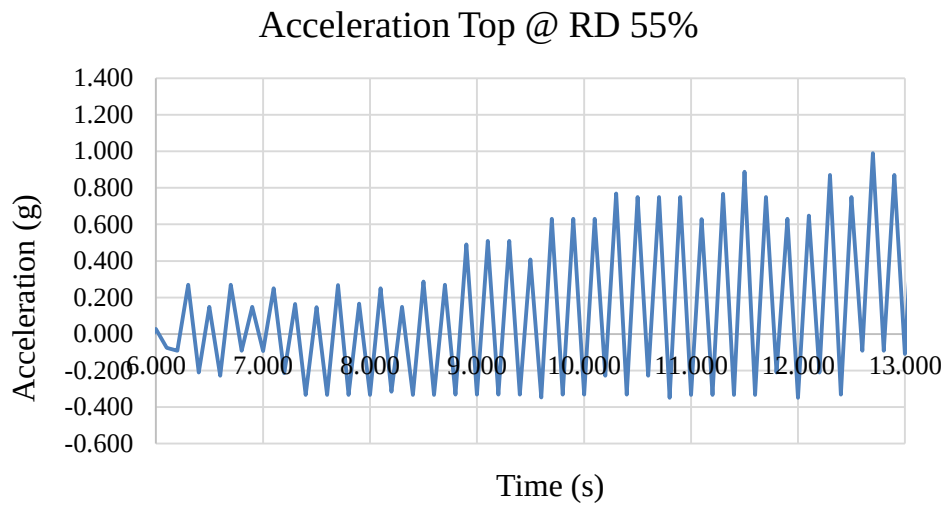

Figure 4.4: Acceleration time history at top of wall (acceleration level 1, R.D. 55%).

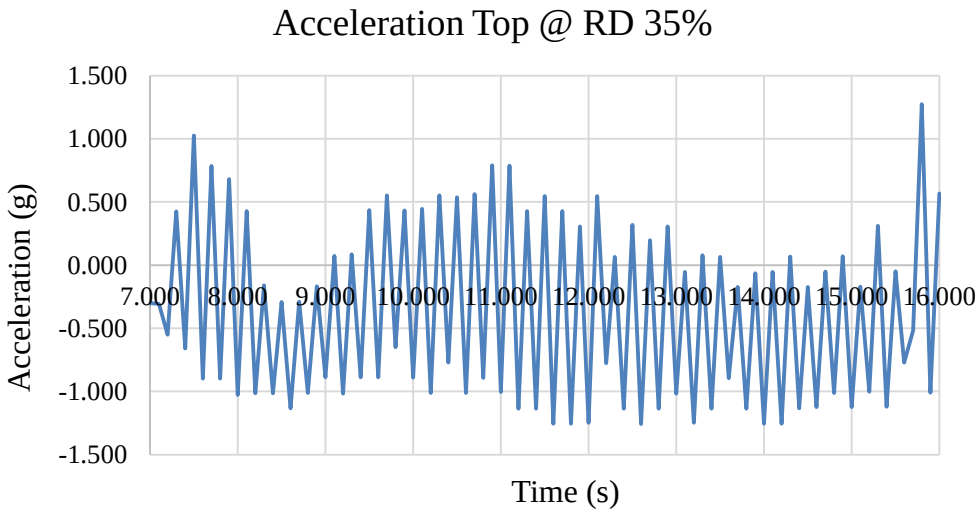

Figure 4.5: Acceleration time history at top of wall (acceleration level 1, R.D. 35%).

The maximum acceleration amplitude in the case of 55 % relative density is 1.224 g which occurs at 14.1 seconds and the maximum amplitude in case of 35 % relative density is 1.377 g and it occurs at 16.5 seconds. Acceleration in case of 45 % relative density is also found to be same and follows the same pattern.

For acceleration 2, the maximum base acceleration amplitude is recorded at 0.843 g. At this base acceleration also, top acceleration is recorded at different densities. The top acceleration response for relative density 55 % is graphically plotted and its time history is shown in adjoining Figure 4.6.

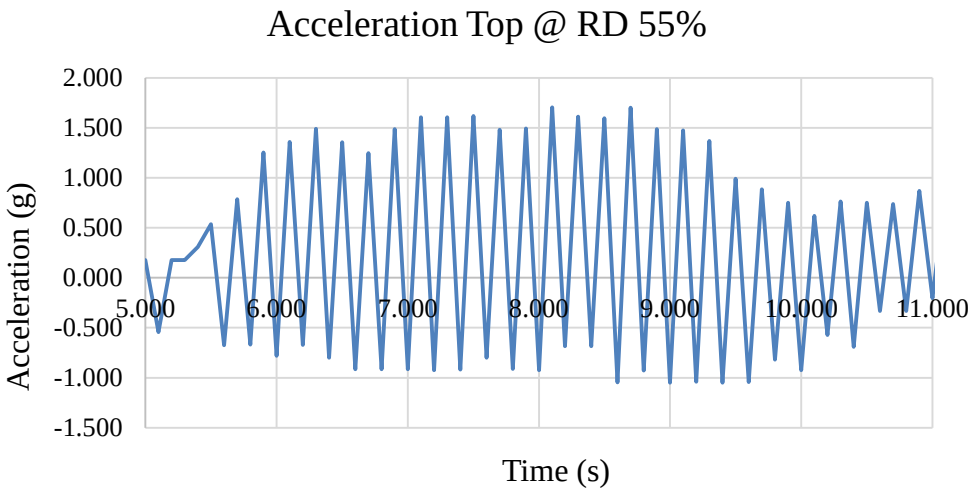

Figure 4.6: Acceleration time history at top of wall (acceleration level 2, R.D. 55%).

The above graph shows the time history for acceleration at the top of the backfill at the relative density of 55%. The maximum amplitude of acceleration is recorded at 1.704 in this case at a time of 8.1 seconds.

At the relative densities of 45% and 35%, the time histories follow the same pattern as in earlier case. For 45% relative density, the maximum amplitude of acceleration is 1.509 g which occurs at 10.8 seconds and for relative density of 35% the maximum amplitude of acceleration is 0.718 g which occurs at 16.8 seconds.

Here we can also see that the maximum amplitude of acceleration at the top of the backfill decreases with decrease in the backfill density of soil i.e. from 1.704 g to 1.509 g to 0.718 g at relative density 55%, 45% and 35% respectively.

In the next case i.e. for acceleration 3, the maximum amplitude of acceleration recorded at base is equal to 0.776. The acceleration response at the top for relative density of 35%, 45% and 55% are recorded. The time histories corresponding to 45% and 35% are graphically plotted and presented in adjoining Figure 4.7 and Figure 4.8 respectively.

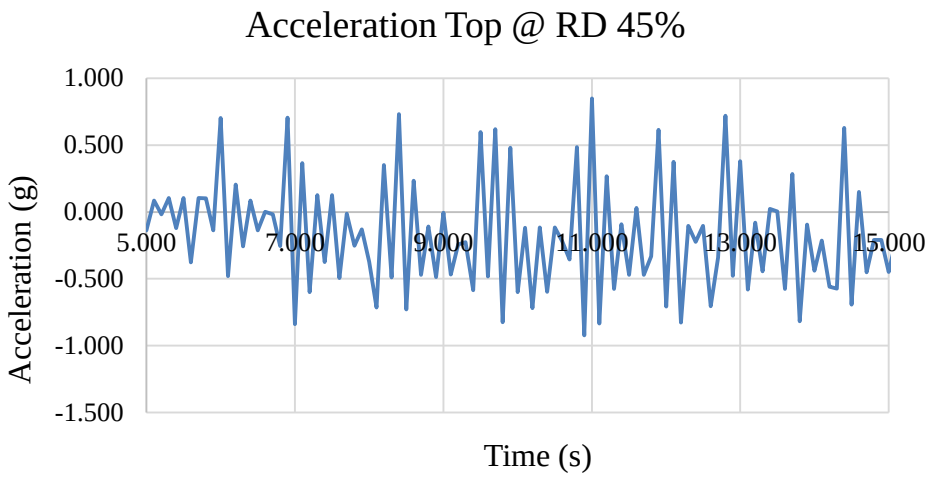

Figure 4.7: Acceleration time history at top of wall (acceleration level 3, R.D. 45%).

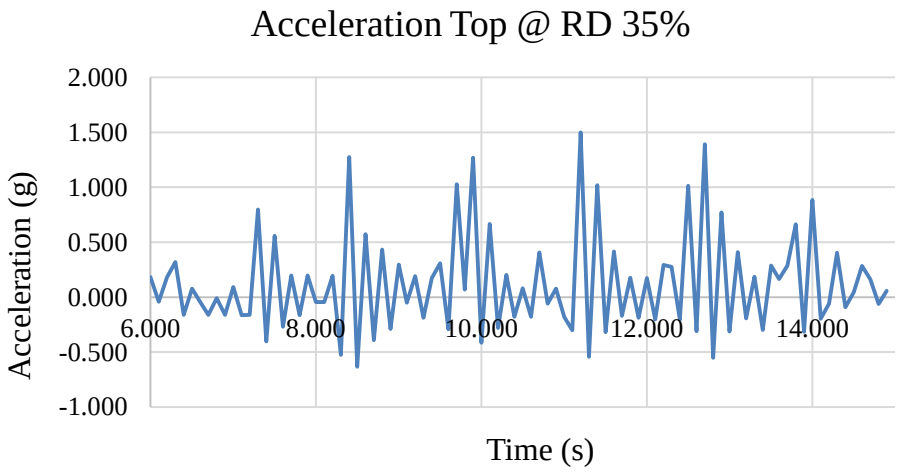

Figure 4.8: Acceleration time history at top of wall (acceleration level 3, R.D. 35%).

From the time histories given in Figure 4.7 and 4.8, the maximum acceleration amplitude at the top of the backfill for R.D. 45% is 0.848 g which occurs at a time of 11 seconds. In the case for backfill R.D. 35%, the maximum acceleration amplitude is 1.499 g which occurs at 11.2 seconds. The time history for 55% R.D. also follows the same pattern.

In the case of base acceleration 3, the maximum acceleration at the top tends to increase with decrease in the relative density of soil.

As shown earlier, the acceleration response at the top of the backfill for rough wall is calculated at three backfill densities and three base accelerations. To estimate the amplification in backfill, ratio between a_{rms} values at top and bottom is calculated for different parametric combinations.

For base acceleration 1, the maximum amplitude of acceleration is recorded at 1.441 g. For this acceleration, the acceleration amplification is as shown in shown in Table 4.1.

Table 4.1: Amplification Ratio for Base Acceleration 1.

RD (%)	**A_{rms} base (g)**	**A_{rms} top (g)**	**Amplification Ratio = A_{rms} top/ A_{rms} base**
55.000	0.845	1.437	1.700
45.000	0.845	0.882	1.044
35.000	0.845	0.810	0.958

From the Table 4.1, we can see that the amplification tends to decrease with decrease in the backfill relative density. The amplification ratio is directly proportional to the relative density of the backfill.

For base acceleration 2, the maximum acceleration amplitude is recorded at 0.843 g. For this amplitude, the acceleration amplification corresponding to different relative density of backfill is given in adjoining Table 4.2.

Table 4.2: Amplification Ratio for Base Acceleration 2.

RD (%)	**A_{rms} base (g)**	**A_{rms} top (g)**	**Amplification Ratio = A_{rms} top/ A_{rms} base**
55.000	0.504	1.009	2.002
45.000	0.504	0.757	1.502
35.000	0.504	0.316	0.627

From the Table 4.2, we can see that it follows the same pattern as in case of acceleration 1 i.e. the amplification ratio decreases with decrease in the R.D. of backfill. Here also the amplification ratio is directly proportional to the R.D. of backfill soil.

For base acceleration 3, the maximum acceleration amplitude is recorded at 0.776 g. For this amplitude, the acceleration amplification corresponding to different relative density of backfill is given in adjoining Table 4.3.

Table 4.3: Amplification Ratio for Acceleration 3.

RD (%)	**A_{rms} base (g)**	**A_{rms} top (g)**	**Amplification Ratio = A_{rms} top/ A_{rms} base**
55.000	0.369	0.165	**0.883**
45.000	0.369	0.469	**1.270**
35.000	0.369	0.516	**1.398**

From the above table we can see that at the acceleration 3, the amplification ratio increases with a decrease in relative density of backfill. This pattern is opposite as compared to pattern followed in acceleration 1 and 2. The amplification ratio is inversely proportional to relative density of backfill in case of acceleration 3.

In this section, it is observed that the both the lateral static and dynamic displacements increase with the increasing in backfill R.D. in most of the cases. At higher acceleration excitation, the acceleration amplification is directly proportional to the relative density of the backfill whereas at lower acceleration excitation, the amplification decreases with increasing in R.D. of backfill. The acceleration response at the top does not follow any specific pattern with change in backfill relative density and it is mostly dependent upon base acceleration excitation.

4.2.2 Effect of base acceleration intensity on dynamic response

In the present study, the experiments are done corresponding to three base accelerations.. The effect of base acceleration on the top acceleration corresponding to three panelled rough wall at varying relative densities is presented. For acceleration 1, the maximum amplitude of base acceleration is 1.441 g. The acceleration time history at the base is as shown in adjoining Figure 4.9.

From the graph in Figure 4.9, we can see that maximum acceleration amplitude is 1.441 g which occurs at 10.7 seconds. For base acceleration 1, the top acceleration varies with variation in backfill relative density.

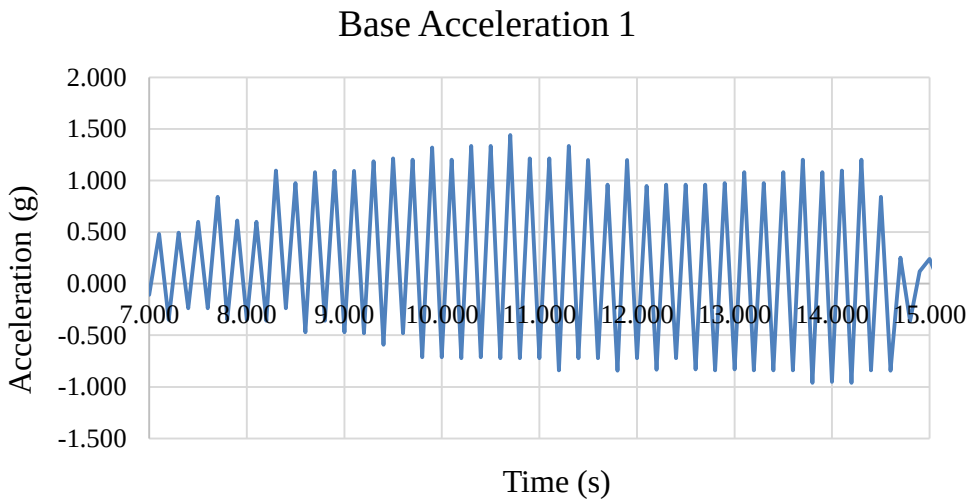

Figure 4.9: Acceleration Level 1 Base Time History.

For acceleration 2, the maximum acceleration amplitude is recorded at 0.843 g. At this base acceleration also, top acceleration is recorded at different densities. Figure 4.10 shows the acceleration 2 base time history.

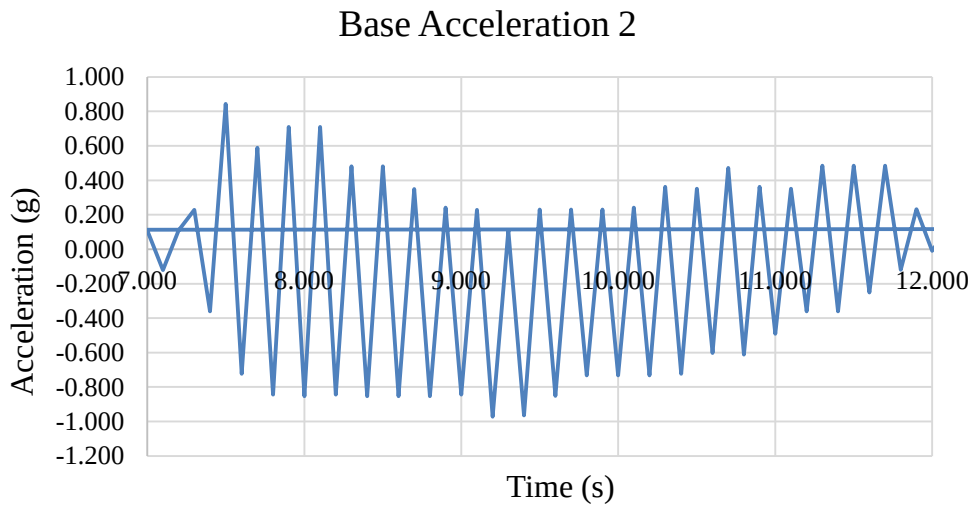

Figure 4.10: Acceleration 2 Base Time History.

The maximum acceleration amplitude of 0.843 g occurs at 7.5 seconds. For acceleration 2 also the top acceleration varies with variation in backfill relative density.

In the next case i.e. for acceleration 3, the maximum amplitude of acceleration recorded at base is equal to 0.776. For this acceleration, the base time history is given in adjoining Figure 4.11.

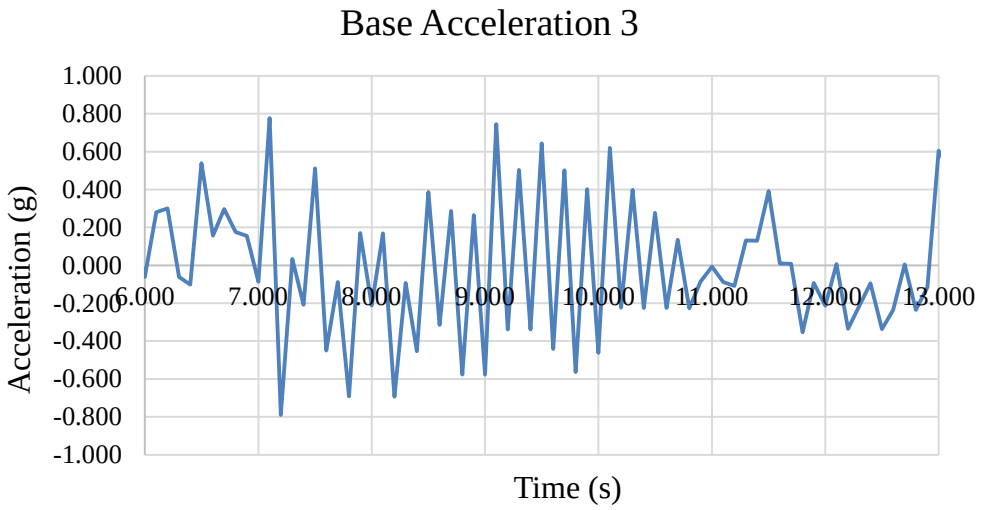

Figure 4.11: Acceleration Level 3 Base Time History.

From the above graph, we can see that the maximum acceleration amplitude i.e. 0.776 g occurs at the time of 7.1 seconds. The acceleration response at the top and lateral displacement response at the middle and top for relative density of 35%, 45% and 55% are recorded.

Displacements are recorded corresponding to three relative densities at different base accelerations i.e. base acceleration 1, 2 and 3. The displacement response varying with base acceleration at a constant relative density is presented in this section. The displacement response corresponding to R.D. 55% is as shown in Figure 4.12.

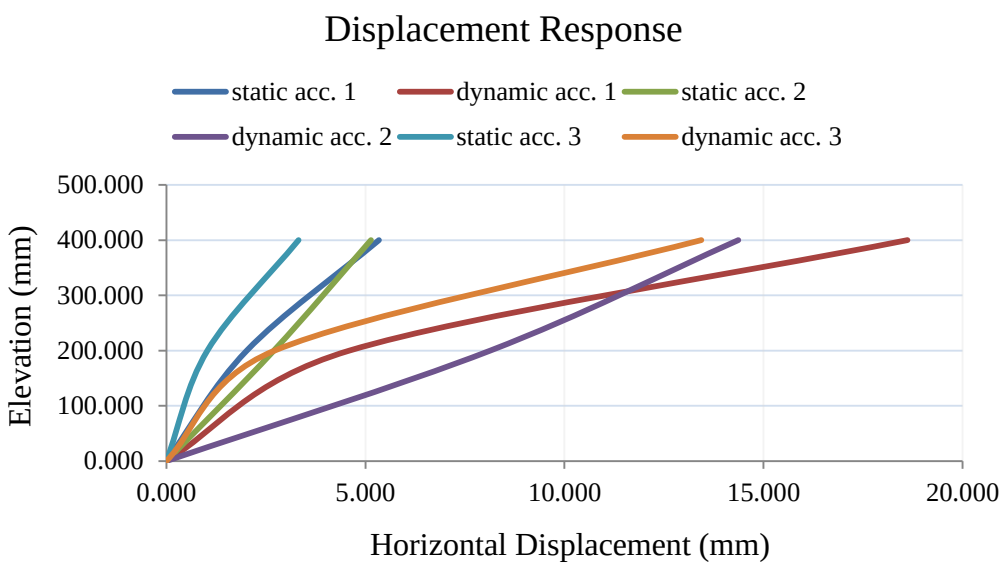

Figure 4.12: *Displacement Response at R.D. 55%.*

From the graph presented in Figure 4.12, we can see that the dynamic displacements are considerably greater than static displacements i.e. about 250 %. The maximum dynamic displacements tend to increase with increasing acceleration amplitude i.e. the maximum displacement occurs at base acceleration 1.

The displacement response corresponding to 45% relative density of backfill is as shown in adjoining Figure 4.13.

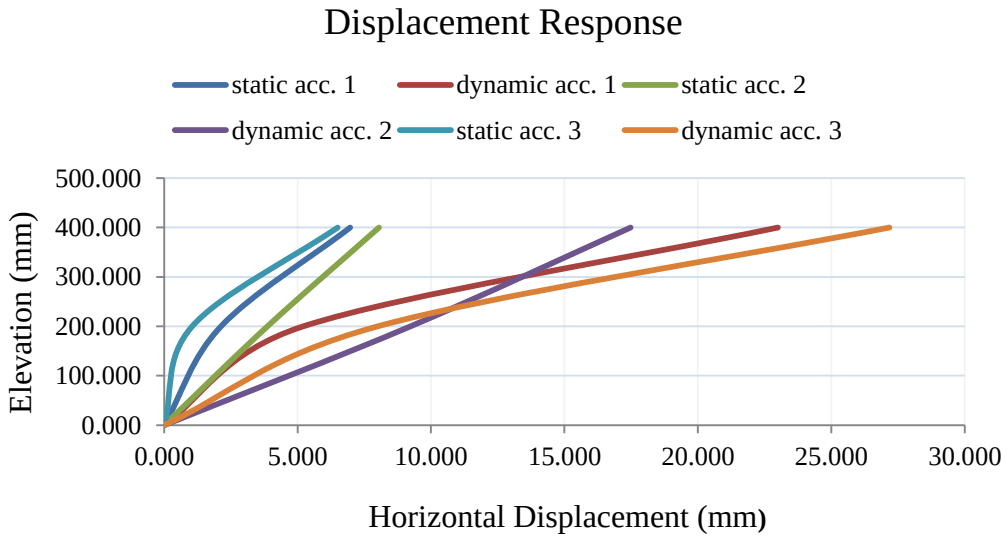

Figure 4.13: *Displacement response at R.D. 45%.*

In this case, almost same pattern is followed as in case of R.D. 55% i.e. the dynamic displacement tends to increase with an increasing base acceleration amplitude and the dynamic displacements are considerably greater than the static displacements i.e. about 221 %.

The static and dynamic displacements corresponding to the R.D. of 35% is as shown in adjoining Figure 4.14.

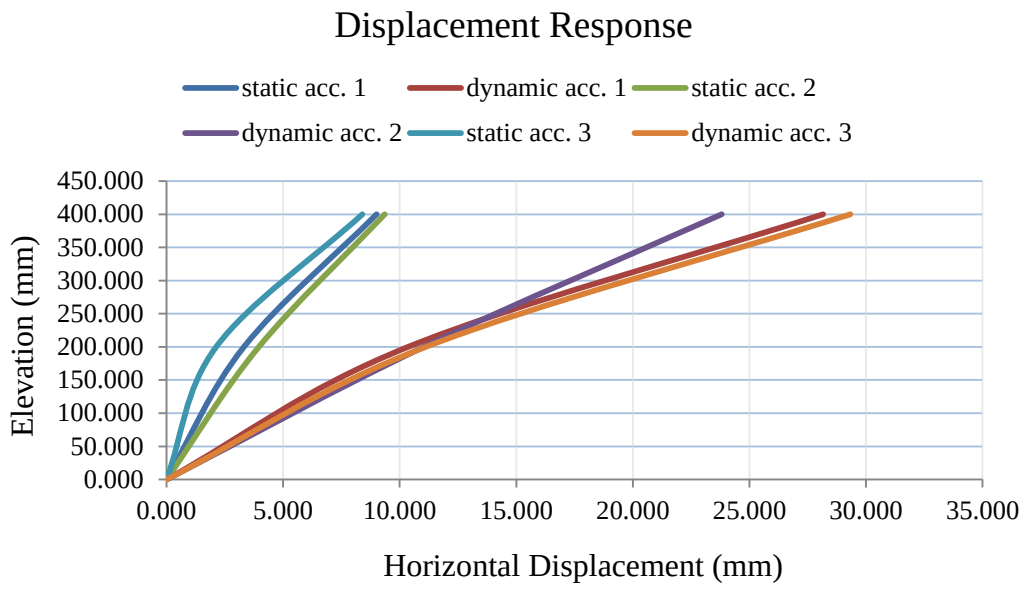

Figure 4.14: *Displacement response at R.D. 35%.*

In the case of R.D. 35%, it can be seen from the graph presented in Figure 4.14 that the static displacements are almost similar and the dynamic displacement slightly increases with increase in acceleration amplitude. The dynamic displacements are about 205 % greater than static displacements.

From the graphs presented in Figures 4.12, 4.13 and 4.14, it can be concluded that dynamic displacements are significantly larger than static displacements. Base acceleration amplitudes also have large effect on the dynamic displacements of the

retaining walls. In most of the cases, the dynamic displacement is directly proportional to the base acceleration amplitude.

In this section, the effect of base acceleration on top acceleration in the backfill is also presented. Accelerations at the top of the backfill are recorded at three R.D. corresponding to varying base accelerations. To estimate the amplification in backfill, ratio between a_{rms} values at top and bottom is calculated for different parametric combinations.

The acceleration amplification corresponding to R.D. 55% at varying acceleration amplitudes is as shown in Table 4.4.

Table 4.4: *Amplification Ratio at R.D. 55%.*

Acceleration	**A_{rms} base (g)**	**A_{rms} top (g)**	**Amplification Ratio = A_{rms} top/ A_{rms} base**
1.000	0.845	1.437	1.700
2.000	0.504	1.009	2.002
3.000	0.369	0.326	0.883

From the above table the acceleration amplification varies with different base accelerations, the amplification is higher for high amplitudes of accelerations and low for lesser acceleration amplitudes.

The acceleration amplification corresponding to R.D. 45% at varying acceleration amplitudes is as shown in Table 4.5.

Table 4.5: Amplification Ratio at R.D. 45%.

Acceleration	A_{rms} base (g)	A_{rms} top (g)	Amplification Ratio = A_{rms} top/ A_{rms} base
1.000	0.845	0.882	1.044
2.000	0.504	0.757	1.502
3.000	0.369	0.469	1.270

The acceleration amplification in case of R.D. 45% occurs maximum at base acceleration level 2. Here also, the acceleration amplification is high for high amplitudes of base acceleration.

The acceleration amplification corresponding to R.D. 35% at varying acceleration amplitudes is as shown in Table 4.6.

Table 4.6: Amplification Ratio at R.D. 35%.

Acceleration	A_{rms} base (g)	A_{rms} top (g)	Amplification Ratio = A_{rms} top/ A_{rms} base
1.000	0.845	0.810	0.958
2.000	0.504	0.316	0.627
3.000	0.369	0.516	1.398

For backfill at R.D. 35%, the maximum acceleration amplification occurs at the base acceleration 3 i.e. the minimum of three accelerations. Here the acceleration amplification decreases with increase in base acceleration amplitude.

We can conclude from the Tables 4.4, 4.5 and 4.6 that the acceleration amplification increases with increase in the base acceleration intensity at high to moderate relative densities of 55% and 45% whereas the amplification decreases with increase in the base acceleration intensity at low relative density of 35%.

4.2.3 Effect of surcharge on top of backfill

In this section, the same rough wall is used as in earlier case and the same test procedure is followed until the sand pluviation. After introducing backfill, a surcharge of 2 kg is kept at a distance of 100 mm from the centre of face of wall. After introducing the surcharge the dynamic displacement is recorded after the application of sinusoidal motion.

In the case of rough wall with surcharge, the static and dynamic displacement is measured at different base acceleration amplitudes of 1.441 g, 0.843 g and 0.776 g. The relative density of backfill was kept constant at 55%. The different lateral static and dynamic displacement at different acceleration amplitudes is detailed and presented in Figure 4.15.

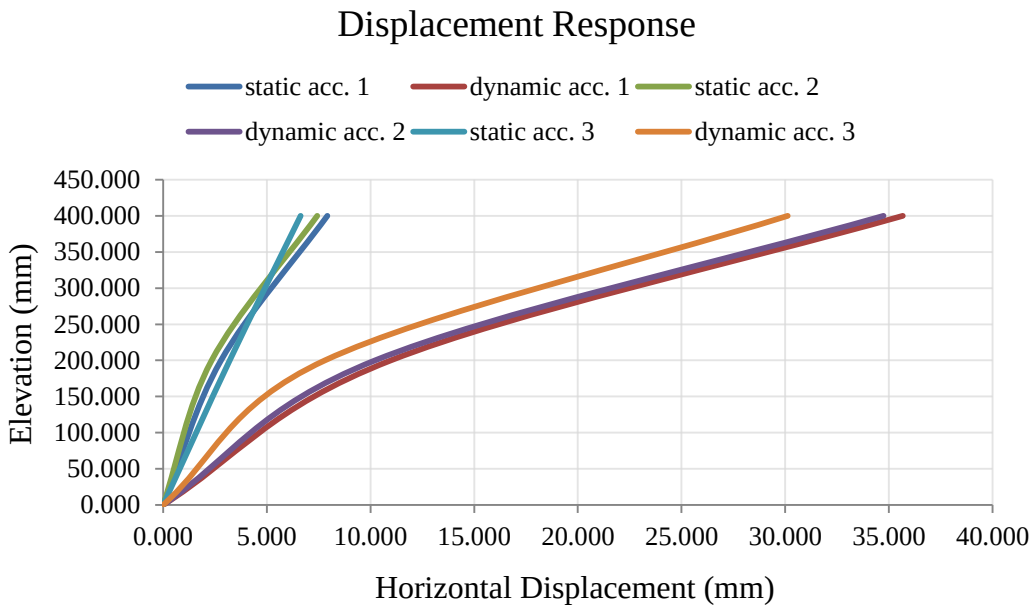

Figure 4.15: Displacement Response at R.D. 55% (surcharge).

From the above graph we can see that the dynamic displacement increases significantly (about 350 %) more than other wall setups as compared to static displacement due to the introduction of surcharge. It can also be seen that with the introduction of surcharge, the maximum displacement does not vary much after the application of different acceleration levels. As for rest of the pattern, it almost remains same as seen earlier in other wall setups. In this section, the comparison between the lateral displacement of this wall with and without surcharge is also presented.

In this sub-section, the displacement comparison is made between rough walls with and without surcharge is presented as follows. The comparison is presented at three base accelerations 1, 2 and 3. For the comparison, the backfill relative density is kept at 55%.

The comparison for base acceleration 1 with maximum amplitude of 1.441 g at 55% relative density of backfill is shown in adjoining Figure 4.16.

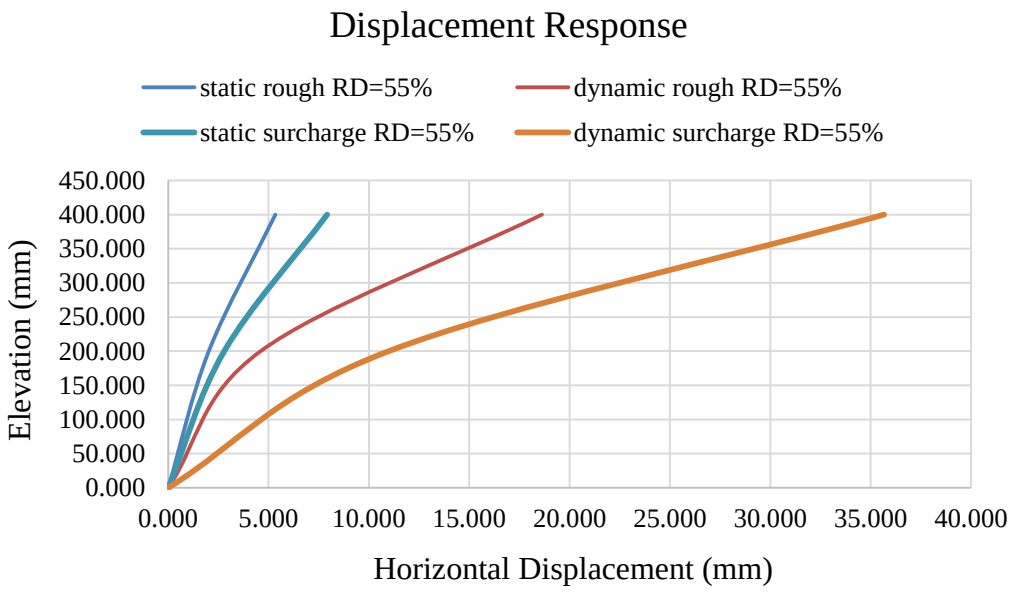

Figure 4.16: Displacement Comparison at Base Acceleration Level 1 (surcharge).

From the above figure, it can be clearly seen that the both the static and dynamic displacement are more in the case of rough wall with surcharge as compared to displacement in rough wall.

For the base acceleration 2 with the maximum amplitude of 0.843 g, the displacement response comparison of rough wall with and without surcharge at backfill density of 55% is given in adjoining Figure 4.17.

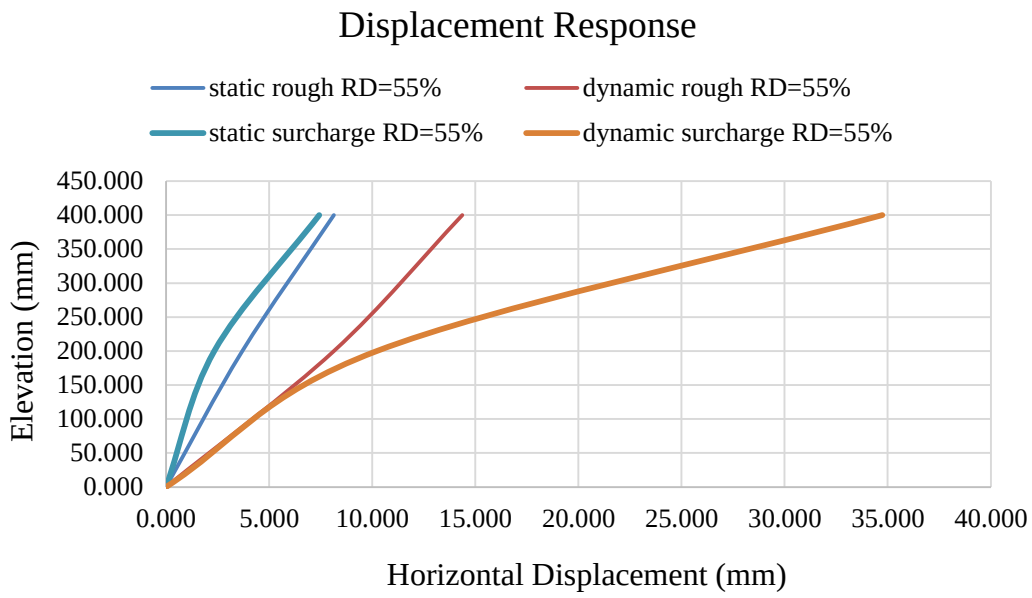

Figure 4.17: Displacement Comparison at Base Acceleration Level 2 (surcharge).

The above comparison also follows the same pattern as seen in previous acceleration i.e. the displacement in rough wall with surcharge is considerably higher than the rough wall without surcharge.

For the base acceleration 3, the displacement response comparison between these two walls at the relative density of 55% is as shown in adjoining Figure 4.18.

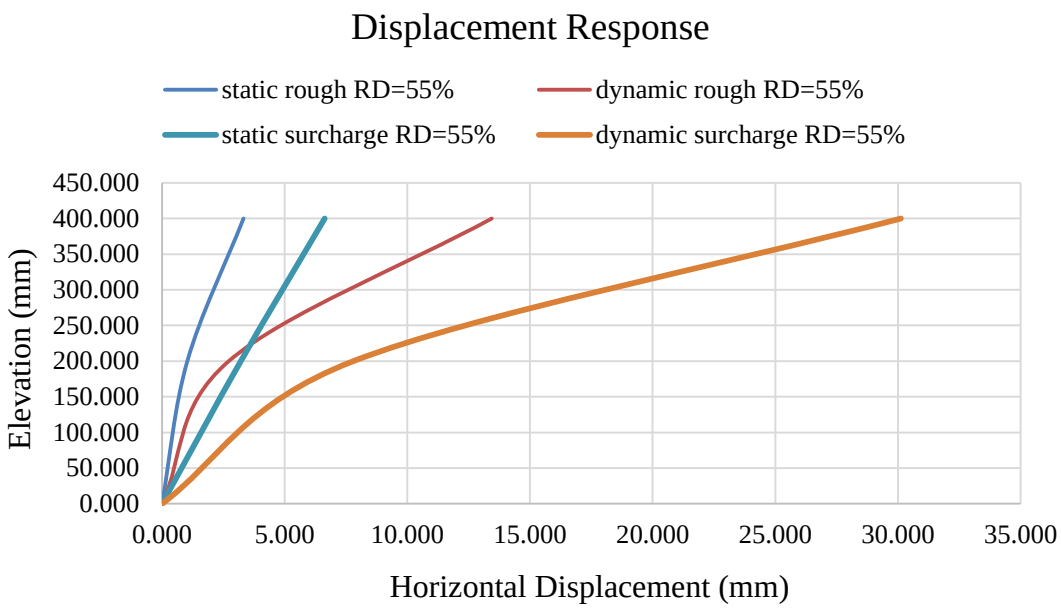

Figure 4.18: Displacement Comparison for Base Acceleration Level 3 (surcharge).

The above graph also follows the same pattern as expected. Both the static and dynamic displacements are considerably higher in case of rough wall with surcharge.

For this wall condition, the top acceleration responses are recorded at base acceleration 1, 2 and 3. The backfill is kept at the relative density of 55% and the acceleration response at the top is recorded corresponding to three base accelerations. The base accelerations time histories are already shown in previous section and the top acceleration time histories corresponding to base accelerations 1, 2 and 3 at relative density of 55% are recorded. The top acceleration time history corresponding to base acceleration 1 is as shown in adjoining Figure 4.19.

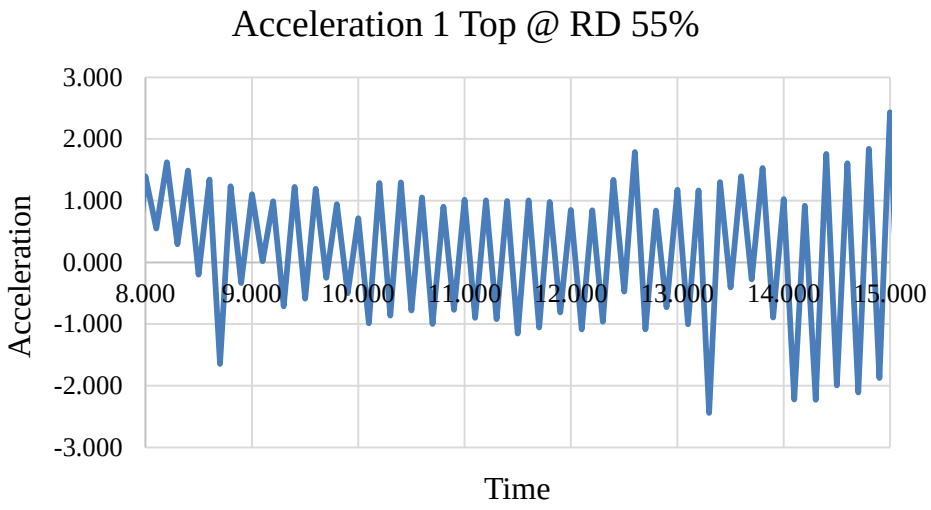

Figure 4.19: Acceleration time history at top of wall (acceleration level 1, R.D. 55%, surcharge).

Corresponding to base acceleration 1, the maximum amplitude of acceleration at the top occurs at time of 15 seconds with amplitude of 2.433 g. The rest of the acceleration level time histories also follow the same pattern as in case of base acceleration 1. Corresponding to base acceleration 2, the maximum amplitude of acceleration at the top occurs at time of 15.2 seconds with amplitude of 2.469 g. For the base acceleration 3, the maximum amplitude of acceleration at the top occurs at time of 12.9 seconds with amplitude of 2.651 g.

From the time histories of rough wall with surcharge at the top corresponding to three base accelerations at R.D. 55%, we can see that the maximum amplitude of acceleration at the top is almost same in all the cases and it slightly increases with the change in base acceleration applied from acceleration 1, 2 and 3 respectively.

In case of rough wall with surcharge, the amplification ratio is calculated for 55% relative density at varying acceleration amplitudes. The acceleration amplification ratio

corresponding to base acceleration 1, 2 and 3 at 55% R.D. of backfill is presented in adjoining Table 4.7.

Table 4.7: Amplification Ratio for R.D. 55%.

Acceleration	**A_{rms} base (g)**	**A_{rms} top (g)**	**Amplification Ratio = A_{rms} top/ A_{rms} base**
1.	0.845	1.068	**1.263**
2.	0.504	1.066	**2.113**
3.	0.369	0.584	**1.584**

From the above table we can see that the acceleration amplification ratio corresponding to acceleration 1 and 3 is almost similar and for acceleration 2, it is slightly higher than other two accelerations.

The acceleration amplification comparison between rough wall and rough wall with surcharge is also presented. The comparison is made at three base acceleration amplitudes at the 55% backfill R.D.

Corresponding to base acceleration levels 1, 2 and 3 with maximum acceleration amplitude of 1.441 g, 0.843 g and 0.776 g respectively, the comparison between rough wall with and without surcharge is presented in adjoining Table 4.8.

Table 4.8: Amplification Ratio Comparison at 55% R.D.

Wall	Base Acceleration Level	A_{rms} base (g)	A_{rms} top (g)	Amplification Ratio = A_{rms} top/ A_{rms} base
Rough wall	1	0.845	1.437	**1.700**
Rough wall with surcharge	1	0.845	1.068	**1.263**
Rough wall	2	0.504	1.009	**2.002**
Rough wall with surcharge	2	0.504	1.066	**2.113**
Rough wall	3	0.369	0.165	**0.883**
Rough wall with surcharge	3	0.369	0.584	**1.584**

From the above table, we can see that the acceleration amplification is generally more in the case of walls with surcharge as compared to same wall without surcharge. This occurs due to the extra load applied by the surcharge on the backfill soil.

From this section, it is observed that the lateral dynamic displacement is significantly more in case of surcharge wall as compared to backfill without surcharge. The acceleration amplification also occurs more in case of surcharge wall in most of the cases with exception of less acceleration amplification in surcharge at higher acceleration excitation.

4.2.4 Effect of interface friction

In this type of wall model, the surface of the wall is made frictionless by affixing smooth sunmica at the backfill facing side of the wall. The same sunmica is used which has been used for making walls of shaking table frictionless. After affixing the sunmica and

following rest of the procedure of performing tests, the lateral displacement at the top and mid of the retaining wall is measured.

In the case of frictionless wall, test is carried out at maximum acceleration amplitude of 0.843 g. The backfill is filled at the relative density of 55%. The lateral displacement is detailed and graphically shown in adjoining Figure 4.20.

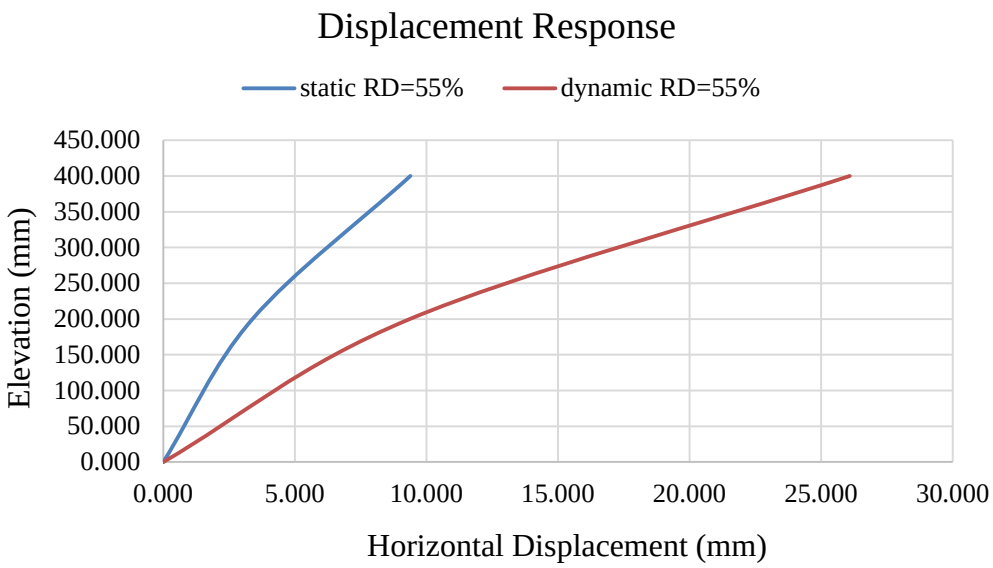

Figure 4.20: Displacement Response at Base Acceleration Level 2 (reduced friction).

From the graph, we can see that the dynamic displacement is significantly greater than static displacement and the maximum displacement occurs at the top of the frictionless wall.

As described in earlier, frictionless wall is made by affixing sunmica over the panels of rough wall. The base acceleration response is same as shown in earlier sections i.e. base acceleration 2. For this wall, acceleration response at top is recorded at 55% relative density. The maximum amplitude of acceleration is 2.772 g which occurs at 9.5 seconds.

The acceleration amplification for frictionless wall is calculated at the backfill relative density of 55% corresponding to the base acceleration 2 which has maximum acceleration amplitude of 0.843 g. the acceleration amplification is given in adjoining Table 4.9.

Table 4.9: Amplification Ratio for Base Acceleration Level 2 (reduced friction).

RD (%)	**A_{rms} base (g)**	**A_{rms} top (g)**	**Amplification Ratio = A_{rms} top/ A_{rms} base**
55.000	0.504	1.220	**2.420**

The amplification ratio is comparatively high in frictionless wall as compared to the amplification in the rough wall as the soil particles are free to move due to reduced friction between them and the wall surface. This also results in higher lateral displacement upon application of sinusoidal motion to the reduced friction models.

4.3 Comparisons between 3 model walls

In this section, comparisons between three model walls i.e. rough wall, reduced friction wall, rough wall with surcharge are made on the basis of acceleration amplification and displacement. The comparisons are made at the relative density of 55% and base acceleration 2.

4.3.1 Amplification Ratio Comparison

In this section, the amplification ratio comparison is made between the three walls at base acceleration 2 corresponding to backfill R.D. of 55%. Comparison is made between the rough wall, frictionless wall and rough wall with surcharge. The comparison between the three walls is as shown in adjoining Table 4.10.

Table 4.10: Amplification Ratio Comparison for Base Acceleration Level 2 (3 walls).

Wall	RD (%)	Arms base (g)	Arms top (g)	ARMS
Rough	55.000	0.504	1.009	**2.002**
Frictionless	55.000	0.504	1.220	**2.420**
Rough with Surcharge	55.000	0.504	1.066	**2.113**

From the above table, we can see that maximum amplification occurs in frictionless wall and the minimum amplification occurs in rough. We can say that with the free movement of soil particles the acceleration amplification increases.

4.3.2 Displacement Comparison

Here the displacement comparison between the three walls used is presented. This displacement comparison is made at base acceleration 2 which has maximum acceleration amplitude of 0.843 g. The displacement corresponding to R.D. 55% is taken for this comparison. It is shown in the adjoining Figure 4.21.

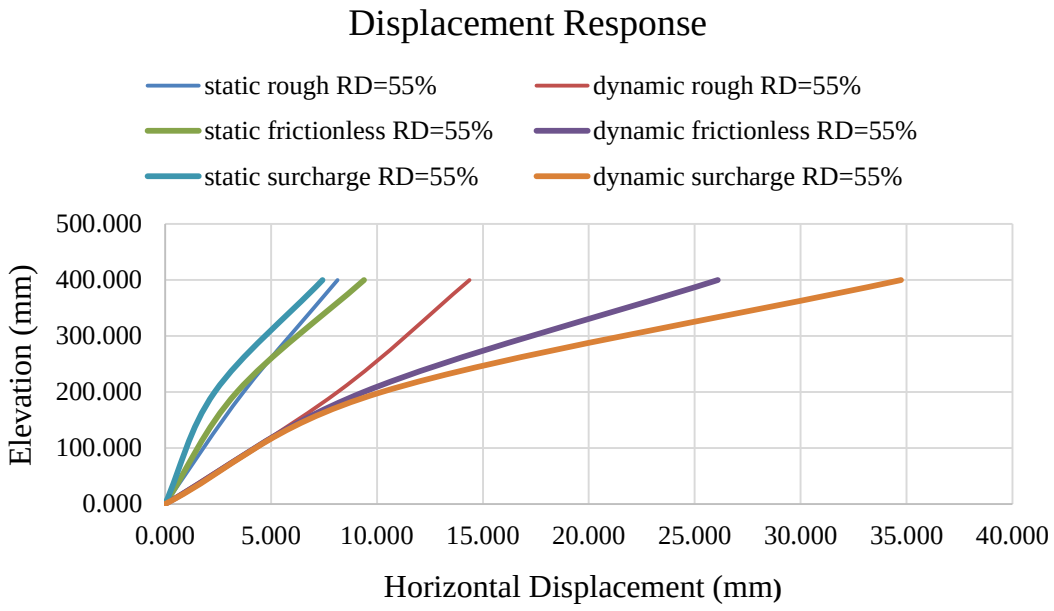

Figure 4.21: Displacement Comparison for Base Acceleration Level 2 (three walls).

From the Figure 4.21, it can be observed that the maximum displacement appears when the surcharge is applied and minimum displacement occurs in the rough wall without surcharge. This happens due to the extra load applied by the surcharge on the backfill of retaining wall which in turn increases the lateral displacement of the wall when sinusoidal motion in applied on the wall. The surcharge applied acts with the sinusoidal motion in increasing the lateral displacement. Frictionless wall also shows more displacement than rough wall as the contact amongst the soil particles and retaining wall is smooth due to which the force exerted on the wall is more as compared to rough wall. The force exerted on the less friction wall is more as the soil particles adjoining the surface of the wall are freer to move as compared to rough wall which offers more friction between the soil particles and the wall facing. Due to more friction between soil particles and wall facing in case of rough wall, the soil particles do not move freely thereby imparting less force as compared to frictionless wall.

4.3.3 Acceleration Amplification Comparison with Literature Present

Comparing the results obtained for acceleration amplification with literature present on tests, Latha et al. (2015) by a sequence of shaking table tests on retaining wall models demonstrated that acceleration amplification does not have any fixed pattern with respect to acceleration intensities and height of the backfill. This observation can be confirmed from the present study. Although, the acceleration amplification varied between 1.1 to 1.3 in the study conducted by Latha et al. (2015) compared to 0.6 to 2 in the present study. This may have occurred due to considerable change in acceleration intensities applied on the models which can be confirmed from study conducted by Latha et al. (2008). In this study, at the higher dynamic excitation the acceleration amplification was found to be higher same as in case of the present study. An increase of amplification at top from 1.71 to 1.91 was observed corresponding to increase in R.D. from 37% to 87%. It has to be

kept in mind that in study done by Latha et al. (2008 & 2015), reinforced backfill was tested, while in present study unreinforced backfill is used and at much higher base accelerations compared to existing literature.

Similarly, comparing the results obtained by Guler & Enunlu (2009), the acceleration amplification varied from 1.21 to 1.9 as compared 0.6 to 2 in the present study. Almost similar range of acceleration amplification has been obtained in the present study. Guler & Enunlu (2009) had a base acceleration of 0.23 g compared to 1.41, 0.843 and 0.776 g in the present study. According to the base acceleration excitation difference in between both the studies, there should have been considerable difference in the range of the acceleration amplification. But we must also note that Guler and Enunlu (2009) used geogrid reinforcements which were not used in the present study due to which the difference in acceleration amplification range is not very pronounced even though the base acceleration used in the present study is considerably high.

Comparing the displacement results obtained by Luciano Oldecop et al. (1996), large amount of displacements were recorded by them at the rate of 10 mm per second. Such great displacements are not recorded in present study as the frequency of base acceleration applied is considerably lower than the magnitude applied by Luciano Oldecop et al. (1996). They had applied the acceleration amplitude of 0.25-1 at a frequency of 10 Hz which is very high as compared to the frequency of 0.8 applied in the present study.

4.4 Theoretical Displacement using Whitman & Liao (1980)

In this section, the results of theoretical displacement computed using Whitman and Liao (1980) approach are presented.

For the validation of the dynamic displacement data records taken by LVDT's, the theoretical maximum displacement due to the appliance of sinusoidal motion at different accelerations is computed using the method given by Whitman & Liao (1980). Theoretical maximum displacement is computed and detailed corresponding to the three panelled rough wall.

For this purpose, the maximum velocity (v_{max}) is assumed and yield acceleration is calculated using the relation proposed by Whitman & Liao (1985) i.e. $a_y/a_{max} \geq 0.4$.

Assuming the maximum velocity (v_{max}) as 0.3 m/s, the theoretical maximum displacements as per Whitman & Liao (1980) corresponding to different base acceleration levels are shown in Table 4.11.

Table 4.11: Theoretical Maximum Displacement at Different Base Accelerations

Maximum Displacement (Whitman & Liao) (1980)			Maximum Experimental Displacement
Base Acceleration (a_{max})	v_{max} (assumed) (m/s)	Dynamic Displacement(mm)	
1.441 g	0.3	5.5	18.62
0.843 g	0.3	9.4	14.37
0.776 g	0.3	10.23	13.44

From the table 4.11, we can see that the theoretical dynamic displacement increases with the decrease in the maximum base acceleration (a_{max}) of the sinusoidal motion applied whereas in case of experimental recorded data, the maximum displacement decreases with decrease in maximum base acceleration of sinusoidal motion. This occurs as the

experimental data is recorded at different backfill densities which considerably affect the lateral displacement of the retaining wall. Whitman and Liao (1980) did not include any parameter in relation to relative density of backfill for the calculation of the maximum displacement. The experimental displacements are also significantly high than theoretical displacements. This may have occurred due to various parameters such as amount of friction between backfill and wall facing, surcharge on the backfill, backfill relative density, confinement of backfill and others which are not included by Whitman and Liao (1980).

CHAPTER 5
CONCLUSIONS AND SUGGESTIONS

5.1 Conclusions

Laboratory experiments were conducted on three different types of retaining wall set ups with backfill sand of grade SP (at R.D. 35 %, 45 % and 55%) using the shaking table at three different base excitations. The conclusions obtained from the obtained results are as follows:

- Achieving the desired backfill density using sand pluviation technique (by using a large sieve of 1.75 mm size) is limited to certain maximum relative density (55% in the present study). After a certain elevation, the height of fall does not have any effect on the change in the density of backfill.
- It is observed by the results of the study that the highest lateral displacement occurs at the top of the wall when the wall is in fixed condition at the bottom.
- Lateral dynamic displacement is more than lateral static displacement both at the top and middle of the retaining wall in all the cases. In case of wall with surcharge, the difference is more pronounced.
- Increasing in the R.D. of backfill resulted in decrease in the lateral wall displacement.
- At high base acceleration amplitudes i.e. at 1.441 g and 0.843 g the acceleration amplification at the top of the backfill increases with an increase in relative density of the backfill.
- For low base acceleration amplitudes i.e. at 0.776 g the acceleration amplification at the top of the backfill decreases with an increase in the relative density of backfill.
- Base acceleration amplitudes also have large effect on the dynamic displacements of the retaining walls. In most of the cases, the dynamic displacement is directly

proportional to the base acceleration amplitude with an exception in case of low R.D. of 35 %.

- The acceleration amplification increases with increase in the base acceleration intensity at high to moderate relative densities of 55% and 45% whereas the amplification decreases with increase in the base acceleration intensity at low relative density of 35%. There is no specific pattern observed in acceleration amplification at varying excitations.
- Comparing the acceleration amplification corresponding to three different walls, the maximum amplification occurs in frictionless wall and the minimum amplification occurs in rough wall. We can say that with the free movement of soil particles the acceleration amplification increases. Although, the acceleration amplification is generally more in the case of walls with surcharge as compared to same wall without surcharge.
- The maximum displacement occurs in case of rough wall with surcharge and minimum displacement occurs in case of rough wall without surcharge. Frictionless wall also shows more displacement than rough wall as the contact between the soil particles and retaining wall is smooth.
- From the theoretical results, we can conclude that the dynamic displacement increases with the increase in the maximum velocity (v_{max}) of the seismic load applied. We can further say that with the decrease in the relative density of soil, the maximum velocity (v_{max}) increases whereas the dynamic displacement increases with the decreasing relative density of soil.

5.2 Comparison with Literature

For the present study, displacement and acceleration results are obtained at varying various parameters. Comparing the results with the previous research works, the base acceleration excitation is varied from 0.776 g to 1.441 g and acceleration amplification obtained in the present study varied from 0.6 to 2 as compared to acceleration

amplification obtained by various researchers such as G. Madhavi Latha et al. (2008 & 2015), who also used the wooden plank wall and recorded acceleration amplification ranging from 0.99 to 1.91 recorded on base excitation of 0.1 g to 0.3 g. Liyan Wang (2015) & A. Komak Panah et al. (2015) recorded an acceleration amplification of 0.5 - 2.4 and 0.9 – 1.7 respectively using concrete blocks as wall facing at base excitation of 0.05 g to 0.5 g. El-Emam et al. (2006) and Luciano Oldecop et al. (1996) also carried out similar research using rigid panel steel wall and acceleration amplification in the range of 1 - 2.8 was recorded by the former at base acceleration excitation of 0.05 g to 0.6.

5.3 Suggestions

From the conclusions, following suggestions are made for the better construction and performance of retaining walls in case of any seismic activity:

- To achieve higher value of backfill R.D., different technique of sand pluviation such as Curtain raining system can be used as presented by Tabaroei et al. (2017).
- To minimize the lateral displacements, elastic geogrid reinforcements can be provided between the backfill and the response can be measured for further study.
- To check the response of modern day retaining walls, concrete block facing retaining wall can be used for further study.
- Saturated sand can be used as the backfill to check the response of pore water pressure on the present study.

REFERENCES

- Al Atik, L., & Sitar, N. (2010). Seismic earth pressures on cantilever retaining structures. Journal of geotechnical and geoenvironmental engineering, 136(10), 1324-1333.

- Bairrao, R., & Vaz, C. (2000, January). Shaking table testing of civil engineering structures–the LNEC 3D simulator experience. In Proceedings 12th World Conference on Earthquake Engineering. Auckland, New Zealand, Paper (Vol. 2129).

- Bathurst, R. J., & Hatami, K. (1998). Seismic response analysis of a geosynthetic-reinforced soil retaining wall. Geosynthetics International, 5(1-2), 127-166.

- Cilingir, U., Haigh, S. K., Madabhushi, S. P. G., & Zeng, X. (2011). Seismic behaviour of anchored quay walls with dry backfill. Geomechanics and Geoengineering, 6(3), 227-235.

- Cai, Z., & Bathurst, R. J. (1995). Seismic response analysis of geosynthetic reinforced soil segmental retaining walls by finite element method. Computers and Geotechnics, 17(4), 523-546.

- Conti, R., Madabhushi, G. S. P., & Viggiani, G. M. B. (2012). On the behaviour of flexible retaining walls under seismic actions. Géotechnique, 62(12), 1081.

- Edgar, T. V., Puckett, J. A., & Rodney, B. D. (1989). Effects of geotextiles on lateral pressure and deformation in highway embankments. Geotextiles and Geomembranes, 8(4), 275-292.

- Elms, D. G., & Richards, R. (1979). Seismic design of gravity retaining walls. University of Canterbury.

- El-Emam, M. M., & Bathurst, R. J. (2004). Experimental design, instrumentation and interpretation of reinforced soil wall response using a shaking table. International Journal of Physical Modelling in Geotechnics, 4(4), 13-32.

- El-Emam, M. M., & Bathurst, R. J. (2007). Influence of reinforcement parameters on the seismic response of reduced-scale reinforced soil retaining walls. Geotextiles and Geomembranes, 25(1), 33-49.

- Geraili Mikola, R., Candia, G., & Sitar, N. (2016). Seismic earth pressures on retaining structures and basement walls in cohesionless soils. Journal of Geotechnical and Geoenvironmental Engineering, 142(10), 04016047.

- Gonçalves, A., Candeias, P., Guerreiro, L., Ferreira, J., & Costa, A. (2016). Characterization of timber masonry walls with dynamic tests. In Historical Earthquake-Resistant Timber Framing in the Mediterranean Area (pp. 299-309). Springer, Cham.

- Guler, E., & Enunlu, A. K. (2009). Investigation of dynamic behavior of geosynthetic reinforced soil retaining structures under earthquake loads. Bulletin of Earthquake Engineering, 7(3), 737-777.

- Hatami, K., & Bathurst, R. J. (2006). Numerical model for reinforced soil segmental walls under surcharge loading. Journal of Geotechnical and Geoenvironmental engineering, 132(6), 673-684.

- Hatami, K., Bathurst, R. J., & El-Emam, M. M. (2005, May). Acceleration amplification in the backfill of reinforced soil walls of different heights. In Proceedings of the 3rd Biot Conference on Poromechanics, University of Oklahoma, Norman (Vol. 6).

- IRC SP 102 (2014) Guidelines for Design and Construction of Reinforced Soil Walls, Indian Road Congress, New Delhi, India.

- IS: 2720-Part III (1980) Determination of specific gravity, Bureau of Indian Standard, New Delhi, India.

- IS: 2720-Part IV (2006) Grain size analysis, Bureau of Indian Standard, New Delhi, India.

- IS: 2720-Part XIII (1986) Direct shear test, Bureau of Indian Standard, New Delhi, India.

- IS: 2720-Part XIV (1983) Determination of density index (relative density) of cohesion less soils, Bureau of Indian Standard, New Delhi, India.

- Kramer, S.L., 1996. Geotechnical Earthquake Engineering. Prentice-Hall, Upper Saddle River, NJ.

- Latha, G. M., & Krishna, A. M. (2008). Seismic response of reinforced soil retaining wall models: influence of backfill relative density. Geotextiles and Geomembranes, 26(4), 335-349.

- Latha, G. M., & Santhanakumar, P. (2015). Seismic response of reduced-scale modular block and rigid faced reinforced walls through shaking table tests. Geotextiles and Geomembranes, 43(4), 307-316.

- Ling, H. I., Liu, H., & Mohri, Y. (2005). Parametric studies on the behavior of reinforced soil retaining walls under earthquake loading. Journal of engineering mechanics, 131(10), 1056-1065.

- Moradi, G. (2014). Seismic response analysis of geosynthetic reinforced soil retaining wall. Electronic Journal of Geotechnical Engineering, 19, 3819-3835.

- Moss, R. E. S., & Noche, R. E. (2012). Scale Model Shake Table Testing of Seismic Earth Pressures in Soft Clay. In GeoCongress 2012: State of the Art and Practice in Geotechnical Engineering (pp. 2078-2087).

- Nelson, A., & Jayasree, P. K. (2010). Seismic Response of Reinforced Soil Retaining Walls with Block Facings.

- Oldecop, L., Zabala, F. R. A. N. C. I. S. C. O., & Almazan, J. L. (1996). Shaking table test on small prototype of soil retaining wall. In Proc. of the 11th World Conf. on Earthquake Engineering. Mexico City.

Panah, A. K., Yazdi, M., & Ghalandarzadeh, A. (2015). Shaking table tests on soil retaining walls reinforced by polymeric strips. Geotextiles and Geomembranes, 43(2), 148-161.

- Richards Jr, R., & Elms, D. G. (1979). Seismic behavior of gravity retaining walls. Journal of Geotechnical and Geoenvironmental Engineering, 105(ASCE 14496).

- Simonelli, A., Carafa, P., Feola, A., Crewe, A. J., & Taylor, C. A. (2000). Retaining walls under seismic actions: shaking table testing and numerical approaches. In XII World Conference on Earthquake Engineering.

- Tabaroei, A., Abrishami, S., & Hosseininia, E. S. (2017). Comparison between two different pluviation setups of sand specimens. Journal of Materials in Civil Engineering, 29(10), 04017157.

- Vieira, C. S., Lopes, M. L., & Caldeira, L. M. M. S. (2006, September). Numerical modelling of a geosynthetic reinforced soil retaining wall subjected to seismic loading. In Proceedings of the 8th International Conference on Geosynthetics, Yokohama, Japan (pp. 1365-1370).

- Wang, L., Chen, G., & Chen, S. (2015). Experimental study on seismic response of geogrid reinforced rigid retaining walls with saturated backfill sand. Geotextiles and Geomembranes, 43(1), 35-45.

- Whitman, R. V., & Liao, S. (1985). Seismic design of gravity retaining walls. Massachusetts Inst of Tech Cambridge Dept of Civil Engineering.

- Whitman, R. V. (1996, June). Designing retaining structures against the effects of earthquakes. In Proc. Vancouver Geotechnical Society Symposium, June (Vol. 7).

- Wood, J. H. (1975). Comments on earthquake-induced soil pressures. In Proceedings of a Workshop on Lateral Earth Pressures and Retaining Wall Design Held During the NZIE Conference, February, 1974 (p. 27). Institution of Professional Engineers New Zealand.

- Zarnani, S., El-Emam, M. M., & Bathurst, R. J. (2011). Comparison of numerical and analytical solutions for reinforced soil wall shaking table tests. Geomechanics and Engineering, 3(4), 291-321.